



Mechanisms of *Trichodesmium* demise within the New Caledonian lagoon during the VAHINE mesocosm experiment

Dina Spungin¹, Ulrike Pfreundt², Hugo Berthelot³, Sophie Bonnet^{3,4}, Dina AlRoumi⁵, Frank Natale⁵, Wolfgang R. Hess², Kay D. Bidle⁵, and Ilana Berman-Frank¹

¹The Mina and Everard Goodman Faculty of Life Sciences, Bar-Ilan University, Ramat-Gan, Israel

²University of Freiburg, Faculty of Biology, Schänzlestr. 1, 79104 Freiburg, Germany

³Aix Marseille Université, CNRS/INSU, Université de Toulon, IRD, Mediterranean Institute of Oceanography (MIO) UM 110, 13288, Marseille, France

⁴Institut de Recherche pour le Développement (IRD), AMU/CNRS/INSU, Université de Toulon, Mediterranean Institute of Oceanography (MIO) UM 110, 13288, Noumea, New Caledonia

⁵Department of Marine and Coastal Sciences, Rutgers University, New Brunswick, NJ, USA

Correspondence to: Ilana Berman-Frank (ilana.berman-frank@biu.ac.il)

Received: 7 December 2015 – Published in Biogeosciences Discuss.: 18 January 2016

Revised: 28 May 2016 – Accepted: 17 June 2016 – Published: 22 July 2016

Abstract. The globally important marine diazotrophic cyanobacterium *Trichodesmium* is abundant in the New Caledonian lagoon (southwestern Pacific Ocean) during austral spring/summer. We investigated the cellular processes mediating *Trichodesmium* mortality from large surface accumulations (blooms) in the lagoon. *Trichodesmium* cells (and associated microbiota) were collected at the time of surface accumulation, enclosed under simulated ambient conditions, and sampled over time to elucidate the stressors and subcellular underpinning of rapid biomass demise (>90% biomass crashed within ~24 h). Metatranscriptomic profiling of *Trichodesmium* biomass, 0, 8 and 22 h after incubations of surface accumulations, demonstrated upregulated expression of genes required to increase phosphorus (P) and iron (Fe) availability and transport, while genes responsible for nutrient storage were downregulated. Total viral abundance oscillated throughout the experiment and showed no significant relationship with the development or demise of the *Trichodesmium* biomass. Enhanced caspase-specific activity and upregulated expression of a suite of metacaspase genes, as the *Trichodesmium* biomass crashed, implied autocatalytic programmed cell death (PCD) as the mechanistic cause. Concurrently, genes associated with buoyancy and gas vesicle production were strongly downregulated concomitant with increased production and high concentrations of transparent exopolymeric particles (TEP). The rapid, PCD-

mediated, decline of the *Trichodesmium* biomass, as we observed from our incubations, parallels mortality rates reported from *Trichodesmium* blooms in situ. Our results suggest that, whatever the ultimate factor, PCD-mediated death in *Trichodesmium* can rapidly terminate blooms, facilitate aggregation, and expedite vertical flux to depth.

1 Introduction

The filamentous N₂-fixing (diazotrophic) cyanobacteria *Trichodesmium* spp. are important contributors to marine N₂ fixation as they form massive blooms (surface accumulations with high biomass density) throughout the oligotrophic marine subtropical and tropical oceans (Capone et al., 1997, 2004; Capone and Carpenter, 1982). These surface blooms with densities of 3000 to >10 000 trichomes L⁻¹ and chlorophyll *a* (Chl *a*) concentrations ranging from 1 to 5 mg L⁻¹ develop swiftly and are characterized by high rates of CO₂ and N₂ fixation (Capone et al., 1998; Luo et al., 2012; Rodier and Le Borgne, 2008, 2010). *Trichodesmium* blooms also occur frequently during austral summer between November and March over large areas of the New Caledonian lagoon in the southwestern Pacific Ocean (Dandonneau and Gohin, 1984; Dupouy et al., 2011).

Trichodesmium has been extensively investigated (reviewed in Capone et al., 1997; Bergman et al., 2012). However, relatively few publications have examined the mortality and fate of these blooms that often collapse abruptly with mortality rates paralleling growth rates and biomass declines > 50 % occurring within 24 h from peak abundance (Bergman et al., 2012; Rodier and Le Borgne, 2008, 2010). Cell mortality can occur due to grazing of *Trichodesmium* by pelagic harpacticoid copepods (O'Neil, 1998) or by viral lysis (Hewson et al., 2004; Ohki, 1999). Both iron (Fe) and phosphorus (P) availability regulate N₂ fixation and production of *Trichodesmium* populations, causing a variety of stress responses when these nutrients are limited (Berman-Frank et al., 2001). Fe depletion, or high light and associated oxidative stress, can also induce in *Trichodesmium* a genetically controlled programmed cell death (PCD) that occurs in both laboratory cultures and in natural populations (Bar-Zeev et al., 2013; Berman-Frank et al., 2004, 2007). Mortality of *Trichodesmium* via PCD is morphologically and physiologically distinct from necrotic death and triggers rapid sinking of biomass that could enhance carbon export in oligotrophic environments (Bar-Zeev et al., 2013). Sinking is due to concomitant internal cellular degradation, vacuole loss, and the increased production of extracellular polysaccharide aggregates, operationally defined as transparent exopolymeric particles (TEP) (Bar-Zeev et al., 2013, 2004; Berman-Frank et al., 2007).

The VAHINE project investigated the fate of newly fixed N by diazotrophs and aimed to test changes in organic matter export, following diazotroph development and mortality. For this, large (50 m³) mesocosms were deployed in the New Caledonian lagoon and followed over the course of 23 days (Bonnet et al., 2016a). Our objective during the VAHINE project was to study the involvement of PCD in the fate of natural *Trichodesmium* blooms induced in these mesocosms. While *Trichodesmium* was initially present, and conditions in the mesocosms appeared favorable, no *Trichodesmium* blooms developed within the mesocosms, yet UCYN-C did increase, allowing for the scientific objectives of the project to be met (Berthelot et al., 2015; Bonnet et al., 2016a; Turk-Kubo et al., 2015). However, *Trichodesmium* developed at different phases of the experimental period outside the mesocosms (Turk-Kubo et al., 2015). Here, we investigated mortality processes in a short-lived *Trichodesmium* bloom that developed and crashed in the lagoon waters at the end of the VAHINE experiment. Using a series of microcosm incubations with collected *Trichodesmium* biomass, we elucidated the stressors and subcellular underpinning of rapid (~24 h) biomass demise and disappearance. Here we present physiological, biochemical, and metatranscriptomic evidence for nutrient-stress-induced PCD in natural populations that leads to *Trichodesmium* mortality, including concomitant down-regulation of gas vesicle synthesis and enhanced TEP production. Such mechanisms would lead to enhanced export flux in natural blooms that also crash within 1–2 days.

2 Methods

2.1 Sampling site and sampling conditions during pre-bloom periods

Our study was performed during the VAHINE mesocosm project set 28 km off the coast of New Caledonia from 13 January 2013 (day 1) to 6 February 2013 in the New Caledonian oligotrophic lagoon (22°29.10' S, 166°26.90' E). The 25 m deep sandy-bottom lagoon is generally protected from the dominant trade winds, yet the waters of the lagoon are influenced by the oligotrophic oceanic waters coming into the lagoon via the Boulari Pass (Bonnet et al., 2016a). Detailed descriptions of the site selection and sampling strategy are provided elsewhere (Bonnet et al., 2016a). The lagoon water outside the mesocosms was sampled daily during the experiment and served as the source for “pre-bloom” data. Throughout the study all noted hours are Noumea local times (LT). Every day, large-volume samples (50 L) were collected from 1, 6, and 12 m depths at 07:00 LT using a Teflon[®] PFA pump and PVC tubing. Samples were immediately transferred back to laboratories aboard the R/V *Alis* and subsampled for a suite of parameters (as described below and in Bonnet et al., 2016a). On day 23 at 12:00, we observed a large surface accumulation of *Trichodesmium* in the lagoon close to the enclosed mesocosms. This biomass accumulation (hereafter called “bloom”) served as the source for experiments 1 and 2 to examine the fate of *Trichodesmium* (Sect. 2.2, Fig. S1 in Supplement).

2.2 Short-term incubations to assess bloom decline

Experiment 1 – *Trichodesmium* filaments and colonies were collected from the dense surface bloom (day 23, 12:00; designated T_0 , Fig. 2a–c) using a plankton net (mesh size, 80 µm) towed through different patches of the bloom from the surface water. The total contents of the net were combined and resuspended in filtered seawater (FSW) (0.2 µm pore size), split between six identical 4.5 L Nalgene polycarbonate bottles (Fig. 2d–e), and incubated as detailed below. Based on previous experience (Berman-Frank et al., 2004), resuspension of *Trichodesmium* cells in the extremely high densities of the surface blooms (> 1 mg L⁻¹ Chl *a*; Fig. 2a–c) would cause an almost immediate crash of the biomass. Consequently, we resuspended the collected biomass in FSW at ~1000-fold lower cell densities (150 µg L⁻¹) that resemble the cellular abundance at the edges of the slicks (Fig. 2). *Experiment 2* – Seawater from the surface bloom was collected 5 h after the initial surface bloom was sighted (day 23, 17:00) by using a Teflon[®] PFA pump and PVC tubing directly filling nine 20 L polyethylene carboys gently to avoid destroying biomass. Bottles from experiments 1 and 2 were placed in on-deck incubators, filled with running seawater to maintain ambient surface temperature (~26 °C), and covered with neutral screening at 50 % surface irradiance levels.

Water from experiment 1 was sampled every 2–4 h for Chl *a* concentration, caspase activity, 16S rRNA gene sequencing, and metatranscriptomics until the biomass collapsed (after ~22 h). Water from experiment 2 was sampled for PON, POC, NH_4^+ , N_2 -fixation rates, TEP production, and virus abundance (days 23–25) (Fig. S1). Prior to incubations, all incubation bottles and carboys were washed with 10 % HCl overnight and rinsed three times with ambient seawater.

2.3 Chlorophyll *a* concentrations

Samples for the determination of Chl *a* concentrations during pre-bloom days were collected by filtering 550 mL of seawater on GF/F filters (Whatman, Kent, UK). Filters were snap-frozen and stored in liquid nitrogen. Chl *a* was extracted in methanol and measured fluorometrically (Herbland et al., 1985), and in experiment 1 measured spectrophotometrically (664 and 750 nm; CARY100, Varian, Santa Clara, CA, USA) according to Tandeau de Marsac and Houmard (1988).

2.4 Particulate organic carbon (POC) and nitrogen (PON)

Detailed POC and PON analyses are described in Berthelot et al. (2015). POC samples were collected by filtering 2.3 L of seawater through precombusted (450 °C, 4 h) GF/F filter and determined using the combustion method (Strickland and Parsons, 1972) on an EA 2400 CHN analyzer. Samples for PON concentrations were collected by filtering 1.2 L of water on precombusted (450 °C, 4 h) and acid-washed (HCl, 10 %) GF/F filters and analyzed according to the wet oxidation protocol described in Pujo-Pay and Raimbault (1994) with a precision of $0.06 \mu\text{mol L}^{-1}$.

2.5 N_2 -fixation rates and NH_4^+ concentrations

N_2 -fixation rate measurements used in experiment 2 are described in detail in Berthelot et al. (2015). Samples were collected at 17:00 in 4.5 L polycarbonate bottles and amended with $^{15}\text{N}_2$ -enriched seawater, within an hour of biomass collection, according to the protocol developed by Mohr et al. (2010) and Rahav et al. (2013). Briefly, seawater was degassed through a degassing membrane (Membrana, Minimodule[®], flow rate fixed at 450 mL min^{-1}) connected to a vacuum pump. Degassed seawater was amended with 1 mL of $^{15}\text{N}_2$ (98.9 % atom ^{15}N , Cambridge Isotopes) per 100 mL. The bottle was shaken vigorously and incubated overnight at 3 bar to promote $^{15}\text{N}_2$ dissolution. Incubation bottles were amended with 1 : 20 (vol : vol) of $^{15}\text{N}_2$ -enriched seawater, closed without headspace with silicone septum caps, and incubated for 24 h under in situ-simulated conditions in on-deck incubators (described above). A total of 2.2 L from each experimental bottle was filtered under low vacuum pressure ($< 100 \text{ mm Hg}$) onto a precombusted (450 °C, 4 h) GF/F filter (25 mm diameter, $0.7 \mu\text{m}$ nominal porosity). The filters were stored at -20 °C and dried for 24 h at 60 °C before

mass spectrometric analysis. PON content and PON ^{15}N enrichments were determined using a Thermo Fisher Scientific Delta Plus isotope ratio mass spectrometer (Bremen, Germany) coupled with an elemental analyzer (Flash EA, Thermo Fisher Scientific). N_2 -fixation rates were calculated according to the equations detailed in Montoya et al. (1996). We assumed significant rates when the ^{15}N enrichment of the PON was higher than 3 times the standard deviation obtained from T_0 samples. The ^{15}N batch did not indicate that our results were overestimated by contamination of the spike solution (Berthelot et al., 2015).

Samples for NH_4^+ were collected in 40 mL glass vials and analyzed by the fluorescence method according to Holmes et al. (1999), using a Trilogy fluorometer (Turner Design).

2.6 Transparent exopolymeric particles (TEP)

Water samples (100 mL) were gently ($< 150 \text{ mbar}$) filtered through a $0.45 \mu\text{m}$ polycarbonate filter (GE Water & Process Technologies). Filters were then stained with a solution of 0.02 % Alcian blue (AB) and 0.06 % acetic acid (pH of 2.5), and the excess dye was removed by a quick deionized water rinse. Filters were then immersed in sulfuric acid (80 %) for 2 h, and the absorbance (787 nm) was measured spectrophotometrically (CARY 100, Varian). AB was calibrated using a purified polysaccharide gum xanthan (GX) (Passow and Alldredge, 1995). TEP concentrations ($\mu\text{g GX equivalents L}^{-1}$) were measured according to Passow and Alldredge (1995).

2.7 Virus abundance

Total seawater (1 mL) was fixed with 0.5 % glutaraldehyde and snap-frozen in liquid nitrogen until processed. Flow cytometry was conducted using an Influx model 209S Mariner flow cytometer and high-speed cell sorter equipped with a 488 nm 200 mW blue laser and two scatter, two polarized, and four fluorescence detectors (BD Biosciences). Viral abundance was determined by staining fixed seawater samples with SYBR Gold (Life Technologies) and measurements of green fluorescence (520, 40 nm band pass). Samples were thawed, diluted 25-fold in $0.22 \mu\text{m}$ filtered Tris/EDTA (TE) buffer (pH 8), stained with SYBR Gold ($0.5\text{--}1 \times$ final concentration), incubated for 10 min at 80 °C in the dark, cooled to RT for 5 min, and mixed thoroughly by vortexing prior to counting on the Influx (Brussaard, 2003). Viral abundance was analyzed using a pressure differential (between sheath and sample fluid) of 0.7, resulting in a low flow rate for higher event rates of virus-like particle (VLP) counts.

2.8 Caspase activity

Biomass was collected on 25 mm, $5 \mu\text{m}$ pore-size polycarbonate filters and resuspended in 0.6–1 mL Lauber buffer (50 mM HEPES (pH 7.3), 100 mM NaCl, 10 % sucrose, 0.1 % 3-(3-cholamidopropyl)-dimethylammonio-1-propanesulfonate, and 10 mM dithiothreitol) and sonicated

on ice (four cycles of 30 s each) using an ultra-cell disruptor (sonic dismembrator, Fisher Scientific, Waltham, MA, USA). Cell extracts were centrifuged ($10\,000 \times g$, 2 min, room temperature) and supernatant was collected for caspase biochemical activity. Caspase-specific activity was determined by measuring the kinetics of cleavage for the canonical fluorogenic caspase substrate (Z-IETD-AFC) at a 50 mM final concentration (using Ex 400 and Em 505 nm; Synergy4 BioTek, Winooski, VT, USA), as previously described in Bar-Zeev et al. (2013). Fluorescence was converted to a normalized substrate cleavage rate using an AFC standard (Sigma) and normalized to total protein concentrations obtained from the same samples. Total protein concentrations were determined by a Pierce™ BCA protein assay kit (Thermo Scientific product #23225).

2.9 16S rRNA gene sequencing and data analyses

Bacterial community diversity was analyzed by deep sequencing of the 16S rRNA gene in samples from two replicate bottles from experiment 1 (see Sect. 2.2) at three time points each. Seawater samples were filtered on 25 mm, 5 µm pore-size Supor filters (Pall Gelman Inc., Ann Arbor, Michigan), snap-frozen in liquid nitrogen, and stored at -80°C for later extraction. Community genomic DNA was isolated from the filters using a phenol–chloroform extraction method modified according to Massana et al. (1997). The 16S rRNA genes within community genomic DNA were initially amplified with conserved bacterial primers 27F and 1100R (Dowd et al., 2008) using a high-fidelity polymerase (Phusion DNA polymerase, Thermo Scientific) with an initial denaturation step of 95°C for 3 min followed by 20 cycles of 95°C for 30 s, 55°C for 30 s, and 72°C for 45 s. A secondary PCR (same conditions) was performed for next-generation sequencing by using customized fusion primers with different tag sequences. The tags were attached to the 27F primer and to the 338R primer (Hamady et al., 2008) to obtain 340 bp fragments suitable for Ion Torrent analysis. Nested PCR was used to minimize inclusion of false sequences into the sequenced material (Dowd et al., 2008). After secondary PCR, all amplicon products were purified using Ampure magnetic purification beads (Agencourt Bioscience Corporation, MA, USA) to exclude primer dimers. The amplicons were sequenced at the Bar-Ilan Sequencing Center, using an Ion Torrent™ (Life Technologies, USA).

The adapter-clipped sequences were processed using tools and scripts from the UPARSE pipeline (Edgar, 2013). Reads from all samples were pooled for operational taxonomic unit (OTU) calling. Reads were de-multiplexed and primers and barcodes were stripped using the script `fastq_strip_barcode_relabel.py`, leaving 42 747 raw reads altogether for six samples. As suggested for OTU calling from single-end amplicon sequences (Edgar, 2013), sequences (mostly between 280 and 300 nt) were trimmed to a fixed length of 280 nt, and shorter sequences were dis-

carded (26 740 trimmed raw reads remained). For OTU clustering, trimmed raw reads were quality-filtered using the `-fastq_filter` command with a maximum expected error rate (`-fastq_maxee`) of 2 (21 590 reads remaining), clustered into unicals (100 % identity) and the unicals sorted by weight (number of sequences in the cluster). OTU clustering with an identity threshold of 0.98 was done using the `-cluster_otus` command on sorted unicals, with built-in chimera filtering. To infer OTU abundances for each individual sample, the trimmed raw reads per sample (after a more relaxed quality filtering with `-fastq_maxee 5`) were mapped back to these OTUs with `-usearch_global` and a minimum identity of 98 %. For taxonomic classification, OTUs were submitted to <https://www.arb-silva.de/ngs/> and classified using the SINA aligner v1.2.10 and database release SSU 123 (Quast et al., 2013). Sequences having (BLAST alignment coverage + alignment identity)/2 < 93 % were considered unclassified and assigned to the virtual group “No Relative” (5.58 % of OTUs).

2.10 RNA extraction and metatranscriptome sequencing

Metatranscriptomic sequencing was performed for three time points: peak surface accumulation of the bloom (T_0 , 12:00), 8 h (T_8 , 22:00), and 22 h (T_{22} , 10:00 the next day) after T_0 . Cells on polycarbonate filters were resuspended in 1 mL PGTX (for 100 mL final volume: phenol 39.6 g, glycerol 6.9 mL, 8-hydroxyquinoline 0.1 g, EDTA 0.58 g, sodium acetate 0.8 g, guanidine thiocyanate 9.5 g, guanidine hydrochloride 4.6 g, Triton X-100 2 mL) (Pinto et al., 2009) with 250 µL glass beads (diameter 0.1–0.25 mm). Cells were subsequently broken on a cell disruptor (Precellys, Peqlab, Germany) at 6500 rpm for 3×15 s at 6500 rpm. Tubes were placed on ice between each 15 s interval. RNA was extracted by adding 0.7 mL chloroform and subsequent phase separation. RNA was precipitated from the aqueous phase using three volumes of isopropanol at -20°C overnight. Residual DNA was removed using the Turbo DNA-free kit (Ambion) according to the manufacturer’s instructions, but adding additional 1 µL of DNase after 30 min of incubation and incubating another 30 min. RNA was purified using Clean & Concentrator 5 columns (C&C 5) (Zymo Research, Freiburg, Germany). The pure RNA was treated with a Ribo-Zero rRNA removal kit (Bacteria) (Epicentre, Madison, USA) and purified again with C&C 5. DNA contamination was tested and confirmed negative with a 40-cycle PCR using cyanobacteria-specific 16S primers.

For removal of tRNAs and small fragments, the RNA was purified with the Agencourt RNAClean XP kit (Beckman Coulter Genomics, Danvers, USA). First-strand cDNA synthesis for T_8 and T_{22} samples was primed with a N6 randomized primer, after which the cDNAs were fragmented by ultrasound (four pulses of 30 s at 4°C). Illumina TruSeq sequencing adapters were ligated in a strand-specific way

to the 5' and 3' ends and the resulting cDNAs were PCR-amplified to about 10–20 ng μL^{-1} using a high-fidelity DNA polymerase. Randomly primed cDNA for T_0 samples was prepared using purified RNA without fragmentation followed by ligation of Illumina TruSeq sequencing adapters to the 5' and 3' ends and fragmentation of cDNA $> \sim 700$ bp with ultrasound (four pulses of 30 s at 4 °C; targeting only cDNA > 700 nt). After repairing ends, fragments were dA-tailed and Illumina TruSeq sequencing adapters were ligated again to the 5' and 3' ends of the cDNA and re-amplified. Consequently, a small fraction of the T_0 reads was not strand-specific. All cDNAs were purified using the Agencourt AM-Pure XP kit (Beckman Coulter Genomics, Danvers, USA) and 2×150 nt paired-end sequences generated with an Illumina NextSeq500 sequencer by a commercial provider (veritis AG, Freising, Germany).

2.11 Bioinformatics processing and analysis of metatranscriptome data

To remove adapters, perform quality trimming, and set a minimal length cutoff, raw fastq reads were processed with Cutadapt version 1.8.1 (Martin, 2011) in paired-end mode with a minimum adapter sequence overlap of 10 nt (-O 10), an allowed error rate of 20 % (-e 0.2) in the adapter sequence alignment, and a minimum base quality of 20. To remove residual ribosomal RNA reads, the fastq files were further processed with SortMeRNA version 1.8 (Kopylova et al., 2012) with the accompanying standard databases in paired-end mode, resulting in 9 469 339 non-ribosomal reads for T_0 , 22 407 194 for T_8 , and 18 550 250 for T_{22} . The fastq files with all non-ribosomal forward reads were used for mapping against the *Trichodesmium erythraeum* IMS101 genome with Bowtie2 (Langmead and Salzberg, 2012) in *very-sensitive-local* mode. This resulted in 51.9 % of T_0 , 5.1 % of T_8 , and 3.3 % of T_{22} reads mapped. Reads were counted per CDS feature as annotated in the genome of *Trichodesmium erythraeum* (NC_008312.1) using htseq-count version 0.6.0 (Anders et al., 2015) and a count table generated with all read counts from T_0 , T_8 , and T_{22} .

For detection of differentially expressed genes from T_0 to T_8 and T_8 to T_{22} , the count table was processed with the statistical tool “Analysis of Sequence Counts” (ASC) (Wu et al., 2010). This tool is specifically designed to account for missing replicates by employing a model of biological variation of gene expression (Wu et al., 2010). The posterior probabilities (P) of a gene being > 2 -fold differentially expressed (user-specified threshold) between any two samples is calculated using an empirical Bayesian analysis algorithm and an internal normalization step. Differential expression of genes was defined as significant if $P > 0.98$.

3 Results

3.1 Setting the scene – *Trichodesmium* bloom development and bloom within the lagoon

Trichodesmium was present as part of the in situ community in the lagoon at the outset of the VAHINE experiment. (Bonnet et al., 2016c; Turk-Kubo et al., 2015). In the lagoon water, temperatures were high (> 25 °C) and typical oligotrophic conditions of austral summer prevailed. For the first 20 days of the experiment low abundance and biomass was measured for primary and secondary production and specifically for diazotrophic populations (Fig. 1). Total PON and POC in the lagoon fluctuated in the first 20 days of the VAHINE experiment with values ranging between 0.6 and 1.1 $\mu\text{mol L}^{-1}$ and 5 and 11 $\mu\text{mol L}^{-1}$, respectively. On the morning of day 23, values were 0.9 and 9.3 $\mu\text{mol L}^{-1}$ PON and POC, respectively (Fig. 1c–d). The total Chl *a* concentrations ranged between 0.18 and 0.26 $\mu\text{g L}^{-1}$ from days 1 to 19 (Fig. 1a). The increase in Chl *a* concentrations reflects the composite signature of the total phototrophic community (detailed in Leblanc et al., 2016; Van Wambeke et al., 2015) and is not specific to *Trichodesmium* biomass. Low abundances of *Trichodesmium* were measured in the lagoon waters throughout the first 3 weeks of the project (Turk-Kubo et al., 2015), with *Trichodesmium*-associated 16S tags ranging from 0.1 to 0.4 % of the total number of 16S tags (Pfreundt et al., 2016). During the first eight days of sampling, *Trichodesmium* abundance, as measured by *nifH* gene real-time PCR, ranged from 3.4×10^2 – 6.5×10^3 *nifH* copies L^{-1} . By days 14 and 16, *Trichodesmium* accounted for 15 % of the total diazotroph population (with 1.1 – 1.5×10^4 *nifH* copies L^{-1}), increasing by day 22 to 42 % of the diazotroph population (1.4×10^5 *nifH* copies L^{-1}) (Turk-Kubo et al., 2015). By the morning of day 23, Chl *a* increased to 0.39 $\mu\text{g L}^{-1}$ in the upper 1 m depth (Fig. 1a), yet *Trichodesmium* was still not visually observed at this time as a bloom on the sea surface. Phycoerythrin concentrations fluctuated between 0.1 and 0.4 $\mu\text{g L}^{-1}$ during days 1–14 and then increased to a maximal peak of $> 0.8 \mu\text{g L}^{-1}$ on day 21 with values $\sim 0.5 \mu\text{g L}^{-1}$ on day 23, reflecting both the doubling in *Synechococcus* biomass (days 15–23) and increasing *Trichodesmium* (days 21–23) (Leblanc et al., 2016). N_2 -fixation rates in the lagoon waters ranged between 0.09–1.2 $\text{nmol N L}^{-1} \text{h}^{-1}$ during the pre-bloom period (Fig. 1c) and on the morning of day 23 were measured at 0.5 $\text{nmol N L}^{-1} \text{h}^{-1}$ (Fig. 1c).

Zooplankton populations in the lagoon fluctuated around 5000 individuals m^{-3} and increased from day 9 to 16, peaking at $\sim 14\,000$ individuals m^{-3} (Hunt et al., 2016). From day 16 to 23 the total zooplankton population declined to ~ 8000 individuals m^{-3} with harpacticoid copepods, including grazers of *Trichodesmium* (*Macrosetella gracilis*, *Miracia efferata*, and *Oculosetella gracilis*), comprising < 1.5 % of total zooplankton community in the lagoon (Hunt et al., 2016). VLP typically ranged from 1 – 6×10^6 mL^{-1} through-

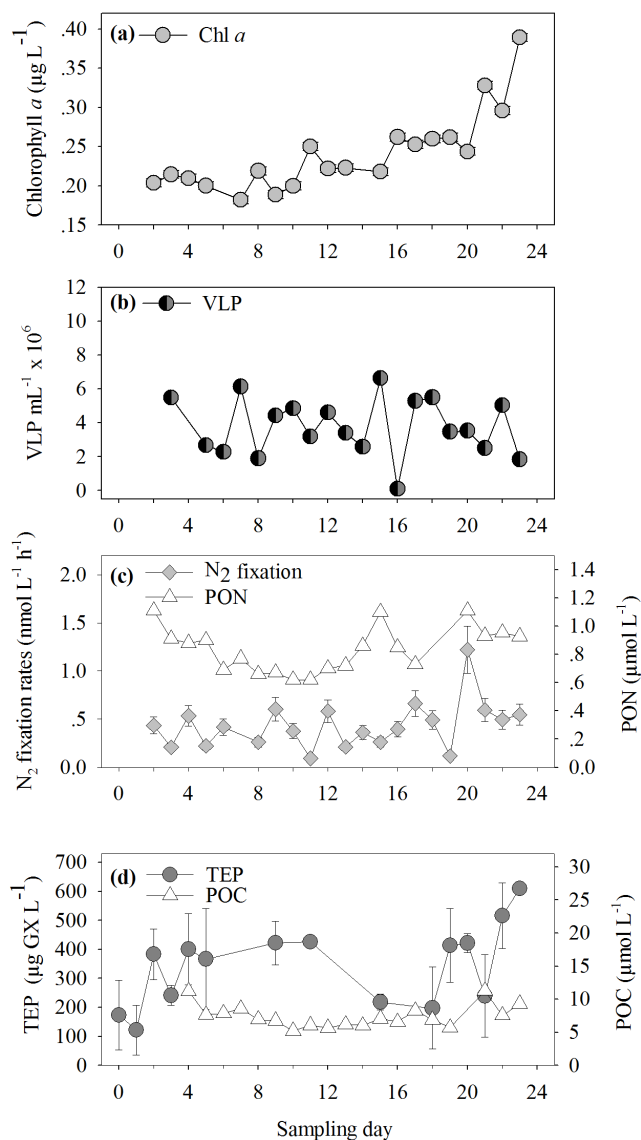


Figure 1. Temporal dynamics of pre-bloom measurements in the lagoon waters. **(a)** Chl *a* concentrations ($\mu\text{g L}^{-1}$). **(b)** Virus-like particles (VLP, $\text{mL}^{-1} \times 10^6$), **(c)** N_2 -fixation rates ($\text{nmol L}^{-1} \text{h}^{-1}$) and particulate organic nitrogen (PON, $\mu\text{mol L}^{-1}$). **(d)** Changes in the concentrations of transparent exopolymeric particles (TEP, $\mu\text{g GX L}^{-1}$) and particulate organic carbon (POC, $\mu\text{mol L}^{-1}$). Water was sampled from the lagoon outside the VAHINE mesocosms, at 1 m depth (surface) throughout the experimental period from day 2 to 23 ($n = 3$). For VLP, the standard error for technical replicates ($n = 3$) was $< 1\%$, which is smaller than symbol size.

out the first 22 days of the VAHINE experiment and displayed a ~ 2 –4-day oscillation (i.e., increasing for 2 days, then declining for the next 3 days, etc.) with mean values of $3.8 \times 10^6 \text{ mL}^{-1}$ (Fig. 1b). VLP counts in surface waters on day 23 were $1.8 \times 10^6 \text{ mL}^{-1}$ (Fig. 1b), just prior to the appearance of the *Trichodesmium* surface bloom. VLP did not show any distinct correlations with total biomass in-

dices such as PON and POC during the pre-bloom sampling (Fig. 1b–d).

Depth-averaged dissolved inorganic phosphorus (DIP) concentrations in the lagoon waters were low, at $0.039 \pm 0.001 \mu\text{M}$, with a relatively stable DIP turnover time (T_{DIP}) of 1.8 ± 0.7 days for the first 15 days, which declined to 0.5 ± 0.7 by day 23 (Berthelot et al., 2015). Alkaline phosphatase activity (APA), which hydrolyzes inorganic phosphate from organic phosphorus, increased ~ 3 -fold, from 1.8 ± 0.7 (average of days 1–4) to $5.0 \pm 1.4 \text{ nmol L}^{-1} \text{h}^{-1}$ (average of days 19–23) (Van Wambeke et al., 2015), demonstrating a response in metabolic activity related to P acquisition for the microbial community probably related to the decreasing availability of DIP in the lagoon waters.

On day 23 (4 February) of the VAHINE measurements, dense surface accumulations of *Trichodesmium* were observed at midday (12:00) (Fig. 2a–c). Ambient air temperatures ($\sim 25^\circ\text{C}$) increased to over 26°C and the winds decreased to $< 5 \text{ kn}$. These accumulations (hereafter blooms) appeared in the typical “slick” formations of dense biomass in ribbons visible on the surface seawater and spread out over tens of meters in the lagoon water outside the mesocosms (Fig. 2a–c). *Trichodesmium* abundance in these patches was extremely variable, with Chl *a* concentrations exceeding 5 mg L^{-1} within dense patches and trichome abundance $> 10\,000$ trichomes L^{-1} . These surface accumulations were visible and sampled again 5 h later (experiment 2), yet by the next morning, no such slicks or patches of dense biomass were observed or measured in the lagoon. The disappearance of the *Trichodesmium* in the lagoon water, whether by drifting away, sinking to depth, or any other factor, prevented further investigation of these populations.

3.2 Investigating *Trichodesmium* mortality in experimental microcosms

3.2.1 Changes in *Trichodesmium* biomass and associated microbial communities

The spatially patchy nature of *Trichodesmium* blooms in the lagoon (Fig. 2a–c), and the rapid temporal modifications in water-column abundance of filaments and colonies probably induced by physical drivers (turbulence and wind-stress), complicate in situ sampling when targeting changes in specific biomass. To overcome this, we collected *Trichodesmium* populations from the surface midday bloom and examined the physiological, biochemical, and gene expression changes occurring with time until the biomass crashed after $\sim 24 \text{ h}$ (see methods Sect. 2.2) (Figs. 2 and 3). In these enclosed microcosms, *Trichodesmium* 16S copies comprised $> 90\%$ of total copies (Fig. 3), enabling the use of Chl *a* to follow changes in its biomass (Fig. 2f). Maximal Chl *a* concentrations in the incubations ($> 150 \pm 80 \mu\text{g L}^{-1}$; $n = 6$) were measured at the start of the incubation soon after the biomass collection and resuspension in FSW. These *Trichodesmium*

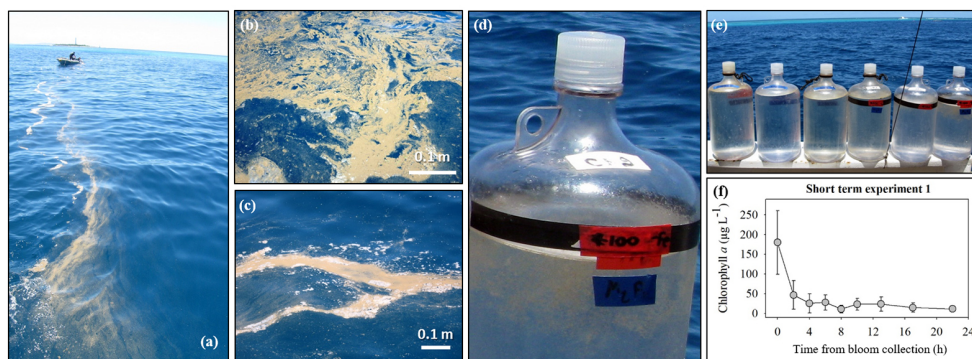


Figure 2. (a–c) Dense surface blooms of *Trichodesmium* observed outside the mesocosms in the lagoon waters on day 23 at 12:00 LT. Photos illustrate the spatial heterogeneity of the surface accumulations and the high density of the biomass. (d–e) To examine the mechanistic of demise (experiment 1), *Trichodesmium* filaments and colonies were collected with a plankton net (mesh size, 80 μm) from the dense surface bloom (day 23, 12:00 LT; designated T_0) and resuspended in 0.2 μm pore-size filtered seawater (FSW) in six 4.5 L bottles. Bottles were incubated on-deck in running-seawater pools with ambient surface temperature ($\sim 26^\circ\text{C}$) at 50 % of the surface irradiance. Bottles were sampled every 2–4 h for different parameters until the biomass crashed. (f) Temporal changes in Chl *a* concentrations in the bottles from the time of biomass collection and resuspension in the bottles until the *Trichodesmium* biomass crashed ~ 24 h after the experiment began ($n = 3$ –6). Photo c. courtesy of A. Renaud.

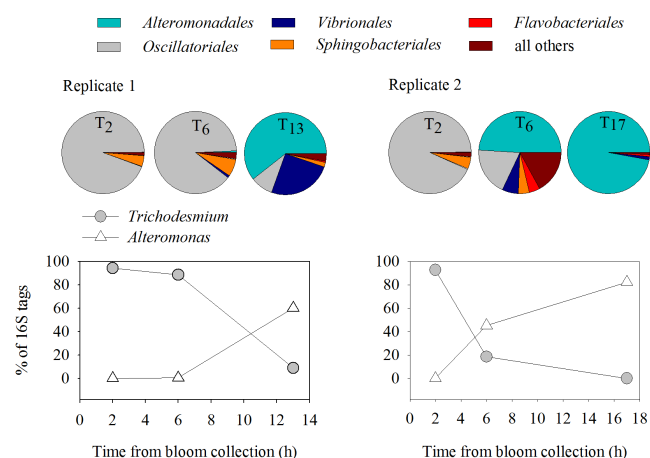


Figure 3. Dynamics of microbial community abundance and diversity during *Trichodesmium* surface bloom as obtained by 16S rRNA gene sequencing for samples collected from the surface waters outside the mesocosms during *Trichodesmium* surface accumulation (bloom) (short-term experiment 1). Pie charts show the changes in dominant groups during the bloom and crash from two replicate incubation bottles (note that Oscillatoriales consisted only of *Trichodesmium* in this experiment). The graphs below show the respective temporal dynamics of *Trichodesmium* (gray circles) and *Alteromonas* (white triangles), the dominant bacterial species during the incubation experiment.

populations collapsed swiftly over the next day, with Chl *a* concentrations declining to 24 and 11 $\mu\text{g L}^{-1}$ Chl *a* after 10 and 22 h, respectively (Fig. 2f).

In experiment 1 we characterized the microbial community associated with the *Trichodesmium* biomass within the microcosms by 16S rRNA gene sequencing from two repli-

cate bottles (experiment 1). At T_0 94 and 93 % of the obtained 16S tags in both replicates (Fig. 3) were of the Oscillatoriales order (phylum Cyanobacteria), with 99.9 % of these sequences classified as *Trichodesmium* spp. (Fig. 3). In both replicates, the temporal decline of *Trichodesmium* biomass coincided with an increase in *Alteromonas* 16S tags, but this development temporally lagged in replicate 1 compared to replicate 2 (Fig. 3). Six hours (T_6) after the surface bloom was originally sampled (T_0), over 80 % of the 16S tags from replicate 1 were characterized as *Trichodesmium*. Fourteen hours after T_0 , Alteromonadales and Vibrionales replaced *Trichodesmium*, thereafter constituting only 9 % of 16S tags (Fig. 3). In replicate 2, *Trichodesmium* declined by 80 % 6 h after T_0 , with Alteromonadales and Flavobacteriales comprising the bulk of the biomass 18 h after the start of incubations (Fig. 3).

The rate of decline in *Trichodesmium* biomass within the 4.6 L microcosms paralleled that of *Trichodesmium* collected from the surface accumulations at 17:00 and incubated in 20 L carboys under ambient conditions for > 72 h (defined hereafter as experiment 2; Fig. 4). Here, *Trichodesmium* biomass decreased by > 80 % within 24 h of incubations with trichome abundance declining from ~ 2500 trichomes L^{-1} at bloom collection to ~ 495 trichomes L^{-1} (Fig. 4a). No direct correlation was observed between the decline of *Trichodesmium* and viral populations. VLP abundance at the time of the surface bloom sampling was at a maximum of $8.2 \times 10^6 \text{ mL}^{-1}$ (Fig. 4a), decreasing to $5.7 \times 10^6 \text{ mL}^{-1}$ in the next 4 h and then remaining stable throughout the crash period (within the next 42 h), averaging $\sim 5 \times 10^6 \pm 0.7 \text{ mL}^{-1}$ (Fig. 4a).

As *Trichodesmium* crashed in the experimental incubations, high values of NH_4^+ were measured (Fig. 4b). In exper-

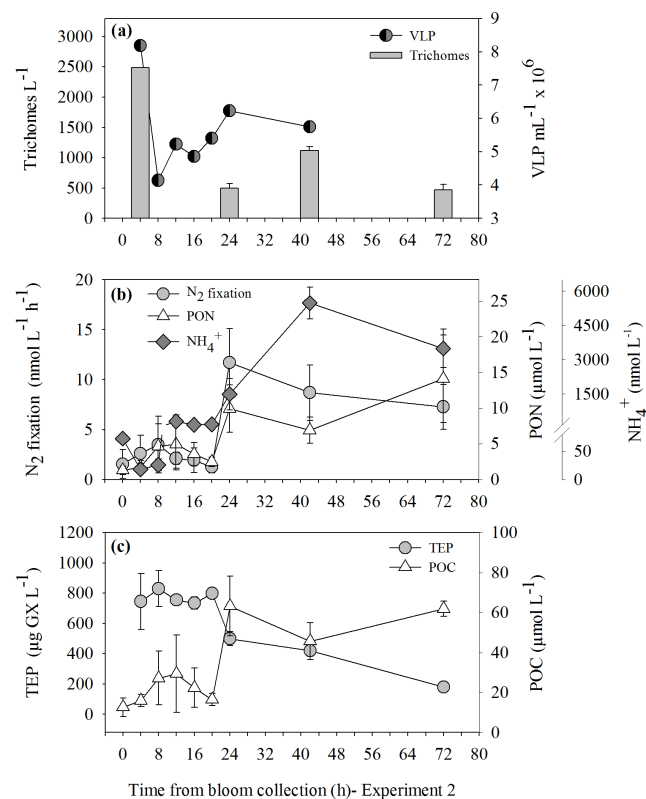


Figure 4. Short-term experiment 2 – measurements from the lagoon waters following *Trichodesmium* bloom on day 23. **(a)** *Trichodesmium* abundance (trichomes L^{-1}) derived from qPCR-based abundances of *Trichodesmium nifH* gene copies (Bonnet et al., 2016b) based on the assumption of 100 gene copies per trichome and virus-like particles (VLP, $mL^{-1} \times 10^6$). **(b)** N_2 -fixation rates ($nmol L^{-1} h^{-1}$), particulate organic nitrogen (PON, $\mu mol L^{-1}$), and ammonium concentrations (NH_4^+ , $nmol L^{-1}$). **(c)** Changes in the concentrations of transparent exopolymeric particles (TEP, $\mu g GX L^{-1}$) and particulate organic carbon (POC, $\mu mol L^{-1}$). For experiment 2, seawater from the surface bloom was collected 5 h after the initial surface bloom was sighted (day 23, 17:00 LT) by directly filling 20 L polyethylene carboys gently to avoid destroying biomass. Bottles were placed in on-deck incubators filled with running seawater to maintain ambient surface temperature ($\sim 26^\circ C$) and covered with neutral screening at 50 % surface irradiance levels. For all parameters, replicates were $n = 3$. For VLP, the standard error for technical replicates ($n = 3$) was $< 1\%$, which is smaller than symbol size.

iment 2, NH_4^+ increased exponentially from $73 \pm 0.4 nmol NH_4^+ L^{-1}$ when the surface bloom was collected and placed in the carboys (17:00) to 1490 ± 686 after 24 h and values $> 5000 nmol L^{-1}$ 42 h after the incubation start (Fig. 4b). The high ammonia declined somewhat by the end of the experiment (after 72 h), yet was still high at $3494 \pm 834 nmol L^{-1}$. Concurrently with the high NH_4^+ concentrations, and despite the dying *Trichodesmium*, we measured an increase N_2 -fixation rates. N_2 fixation rose from 1.5 at T_0 to

$3.5 \pm 2.8 nmol NL^{-1} h^{-1}$ 8 h after incubations began and $11.7 \pm 3.4 nmol NL^{-1} h^{-1}$ 24 h later (Fig. 4b). These high values represent other diazotrophs including UCYN types and diatom–diazotroph associations that flourished after the *Trichodesmium* biomass had declined in the carboys (Bonnet et al., 2016b; K. Turk-Kubo, personal communication, 2016). POC and PON, representing the fraction of C and N incorporated into biomass, ranged between 5.2 and $11.2 \mu mol CL^{-1}$ and 0.6 and $1.1 \mu mol NL^{-1}$ during pre-bloom periods (Fig. 1c–d) and $12.6 \pm 4.6 \mu mol CL^{-1}$ and $1.3 \pm 0.5 \mu mol NL^{-1}$ when the surface bloom was sampled (Fig. 4b–c). Twenty-four hours after collection of bloom biomass, POC increased ~ 6 -fold to $63.2 \pm 15 \mu mol CL^{-1}$ and PON increased 10-fold to $10 \pm 3.3 \mu mol NL^{-1}$ (Fig. 4b–c). After 72 h, total POC was $62 \pm 4 \mu mol CL^{-1}$ (Fig. 4c) and PON increased to $14.1 \pm 6 \mu mol NL^{-1}$ (Fig. 4b).

Organic carbon in the form of TEP is secreted when *Trichodesmium* is stressed and undergoing PCD (Bar-Zeev et al., 2013; Berman-Frank et al., 2004). TEP concentrations in the lagoon waters during the pre-bloom period (first 20 days) fluctuated around $\sim 350 \mu g GX L^{-1}$ (Fig. 1d) that increased to $\sim 500 \mu g GX L^{-1}$ on day 22 (Fig. 1d). During the time of biomass collection from the surface bloom TEP concentration exceeded $700 \mu g GX L^{-1}$ (Fig. 4c). After biomass enclosure (experiment 2) TEP concentrations declined to $420 \pm 35 \mu g GX L^{-1}$ and subsequently to $180 \pm 25 \mu g GX L^{-1}$ 42 h and 72 h after T_0 (Fig. 4c).

3.2.2 Genetic responses of stressed *Trichodesmium*

Metatranscriptomic analyses of the *Trichodesmium* biomass were conducted in samples from experiment 1, at T_0 , T_8 , and T_{22} (Fig. S1). We examined differential expression during this period by investigating a manually curated gene suite including specific pathways involved in P and Fe uptake and assimilation, PCD, or gas vesicle synthesis. Genes involved in the acquisition and transport of inorganic and organic P sources were upregulated, concomitant with biomass demise; significantly higher expression levels were evident at T_8 and T_{22} compared to T_0 (Table S1). Abundance of alkaline phosphatase transcripts, encoded by the *phoA* gene (Orchard et al., 2003), increased significantly (~ 5 -fold) from T_0 to T_{22} (Fig. 5a). The transcript abundance of phosphonate transporters and C-P lyase genes (*phnC*, *phnE*, *phnH*, *phnI*, *phnL*, and *phnM*) increased significantly (5–12-fold) between T_0 and both T_8 and T_{22} (Fig. 5a, Table S1). Of the phosphite uptake genes, only *ptxA* involved in the phosphite (reduced inorganic phosphorus compound) uptake system, and recently found to operate in *Trichodesmium* (Martínez et al., 2012; Polyviou et al., 2015), was significantly upregulated at both T_8 and T_{22} compared to T_0 (4.5- and 7-fold change, respectively). The two additional genes involved in phosphite uptake, *ptxB* and *ptxC*, did not change significantly, as *Trichodesmium* biomass crashed (Fig. 5a).

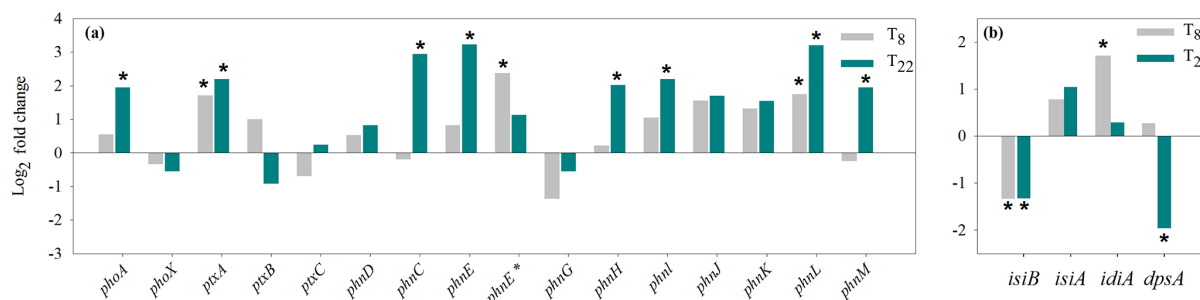


Figure 5. (a) Expression of alkaline phosphatase associated genes *phoA* and *phoX* (Tery_3467 and Tery_3845); phosphite utilization genes *ptxA*, *ptxB*, and *ptxC* (Tery_0365, Tery_0366, and Tery_0367); and phosphonate utilization genes (*phn* genes, Tery_4993, Tery_4994, Tery_4995, Tery_4996*, Tery_4997, Tery_4998, Tery_4999, Tery_5000, Tery_5001, Tery_5002 and Tery_5003). Asterisks near locus tag numbers indicate gene duplicates. (b) Iron-related genes, *isiB* (Tery_1666), *isiA* (Tery_1667), *idiA* (Tery_3377), and ferritin DPS gene *dpsA* (Tery_4282). Bars represent log₂-fold changes of corresponding genes at T₈ (8 h after T₀) and T₂₂ (22 h after T₀) in comparison to T₀. A significant change in expression from T₀ was tested with ASC (Wu et al., 2010) and marked with an asterisk. A gene was considered differentially expressed if $P > 0.98$ (posterior probability).

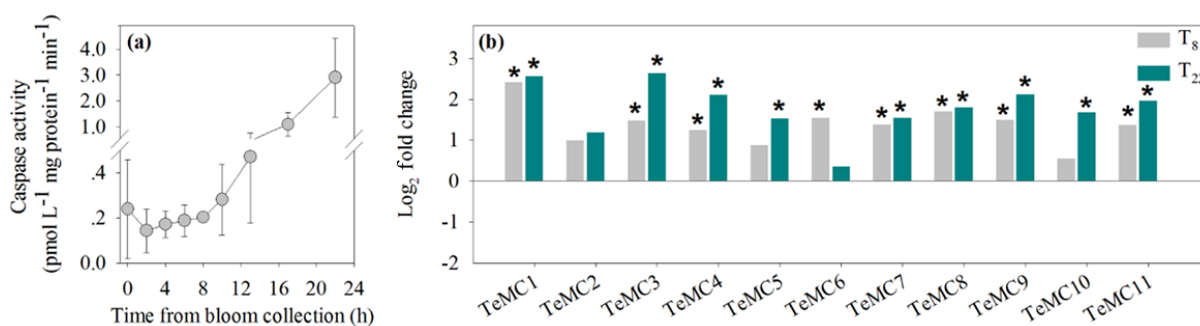


Figure 6. (a) Dynamics of caspase-specific activity rates (pmol L⁻¹ mg protein⁻¹ min⁻¹) of *Trichodesmium* in the New Caledonian lagoon during bloom accumulation and bloom demise, sampled during experiment 1. Samples ($n = 6$) collected from the bloom (day 23, 12:00 LT, T₀) were incubated on-deck in an incubator fitted with running seawater to maintain ambient surface temperature (see Methods). (b) Transcript accumulation of metacaspase genes in the *Trichodesmium* bloom during the short-term incubation experiment. Metacaspase genes are TeMC1 (Tery_2077), TeMC2 (Tery_2689), TeMC3 (Tery_3869), TeMC4 (Tery_2471), TeMC5 (Tery_2760), TeMC6 (Tery_2058), TeMC7 (Tery_1841), TeMC8 (Tery_0382), TeMC9 (Tery_4625), TeMC10 (Tery_2624), and TeMC11 (Tery_2158). Bars represent log₂-fold changes at T₈ (8 h after T₀) and T₂₂ (22 h after T₀) in comparison to T₀. Significant change in expression from T₀ was tested with ASC (Wu et al., 2010) and marked with an asterisk. A gene was considered differentially expressed if $P > 0.98$ (posterior probability).

As Fe limitation induces PCD in *Trichodesmium* (Berman-Frank et al., 2004, 2007), we examined genetic markers of Fe stress. At the time of surface bloom sampling (experiment 1, T₀), Fe stress was indicated by higher differential expression of several genes. The *isiB* gene encodes flavodoxin and serves as a common diagnostic indicator of Fe stress in *Trichodesmium*, since it may substitute for Fe-S-containing ferredoxin (Bar-Zeev et al., 2013; Chappell and Webb, 2010). Transcripts of *isiB* were significantly higher at T₀ (3-fold) than at T₈ and T₂₂ (Fig. 5b, Table S1). The chlorophyll-binding protein *IsiA* is induced in cyanobacterial species under Fe or oxidative stress to prevent oxidative damage (Laudenbach and Straus, 1988). Here *isiA* transcripts increased 2- and 3-fold from T₀ to T₈ and T₂₂, respectively (Fig. 5b, Table S1). The Fe transporter gene *idiA* showed a transient higher transcript accumulation only at T₈.

As the health of *Trichodesmium* declined, transcripts of the Fe-storage protein ferritin (*Dps*) decreased by > 70 % at T₂₂ (Fig. 5b, Table S1)

3.2.3 PCD-induced demise

Our earlier work demonstrating PCD in *Trichodesmium* allowed us to utilize two independent biomarkers to investigate PCD induction during *Trichodesmium* demise, namely changes in catalytic rates of caspase-specific activity (Berman-Frank et al., 2004, 2007) and levels of metacaspase transcript expression (Bar-Zeev et al., 2013). When the surface bloom was sampled (experiment 1, T₀), protein normalized caspase-specific activity was very low at 0.23 ± 0.2 pmol L⁻¹ mg protein⁻¹ min⁻¹ (Fig. 6a). After a slight decline in the first 2 h, caspase activity increased throughout the experiment with 10-fold higher val-

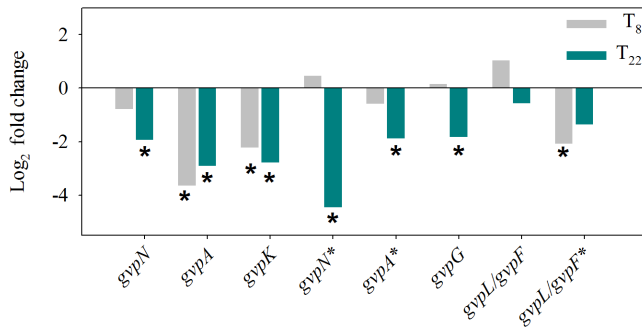


Figure 7. Change in gas vesicle protein (*gvp*) genes as obtained from metatranscriptomic analyses of the *Trichodesmium* bloom from peak to collapse (experiment 1). *gvpA* genes (Tery_2330 and Tery_2335*) encode the main constituent of the gas vesicles that forms the essential core of the structure; *gvpN* (Tery_2329 and Tery_2334*), *gvpK* (Tery_2322), *gvpG* (Tery_2338), and *gvpL/gvpF* (Tery_2339 and Tery_2340*) encode vesicle synthesis proteins. Asterisks near locus tag numbers indicate gene duplicates. Bars represent log₂-fold changes at T₈ (8 h after T₀) and T₂₂ (22 h after T₀) in comparison to T₀. Significant change in expression from T₀ was tested with ASC (Wu et al., 2010) and marked with an asterisk. A gene was considered differentially expressed if $P > 0.98$ (posterior probability).

ues ($2.9 \pm 1.5 \text{ pmol L}^{-1} \text{ mg protein}^{-1} \text{ min}^{-1}$) obtained over the next 22 h as the bloom crashed (Fig. 6a).

We followed transcript abundance over the demise period for the 12 identified metacaspase genes in *Trichodesmium* (Asplund-Samuelsson et al., 2012; Asplund-Samuelsson, 2015; Berman-Frank et al., 2004): TeMC1 (Tery_2077), TeMC2 (Tery_2689), TeMC3 (Tery_3869), TeMC4 (Tery_2471), TeMC5 (Tery_2760), TeMC6 (Tery_2058), TeMC7 (Tery_1841), TeMC8 (Tery_0382), TeMC9 (Tery_4625), TeMC10 (Tery_2624), TeMC11 (Tery_2158), and TeMC12 (Tery_2963) (Fig. 6b, Table S1). A subset of these genes was previously shown to be involved in PCD of *Trichodesmium* cultures in response to Fe and light stress (Bar-Zeev et al., 2013, 2004; Bidle, 2015). Here, we interrogated the entire suite of metacaspases in natural *Trichodesmium* populations. As the biomass crashed from T₀ to T₂₂, 7 out of 12 metacaspases (TeMC1, TeMC3, TeMC4, TeMC7, TeMC8, TeMC9, and TeMC11) were significantly upregulated 8 and 22 h after T₀ (Fig. 6b). For these genes, transcript abundance increased 2.3- to 5.3-fold 8 h after T₀ and 3.5–6.2-fold 22 h after T₀ (Fig. 6b, Table S1) TeMC5 and TeMC10 transcripts increased significantly after 22 h by 2.9- and 3.2-fold, respectively. TeMC6 was upregulated 2.9-fold after 8 h. TeMC2 transcripts did not significantly change over time. We did not detect any expression of TeMC12 throughout the experiment.

Export flux can be enhanced by PCD-induced sinking (Bar-Zeev et al., 2013) as PCD in *Trichodesmium* results in degradation of internal components, especially gas vesicles that are required for buoyancy (Berman-Frank et al., 2004).

Although we did not measure changes in buoyancy itself, we observed rapid sinking of the *Trichodesmium* biomass in the bottles and carboys. The metatranscriptomic analyses demonstrated that, excluding one copy of *gvpL/gvpF*, gas vesicle protein (*gvp*) genes involved in gas vesicle formation (*gvpA*, *gvpN*, *gvpK*, *gvpG*, and *gvpL/gcpF*) were all significantly downregulated relative to T₀ (Fig. 7, Table S1).

4 Discussion

4.1 Mortality processes of *Trichodesmium* – incubation results

4.1.1 Grazer and virus influence

Our microcosm incubations allowed us to specifically focus on the loss factors and show the involvement of biotic and abiotic stressors in inducing PCD and mechanistically impacting the demise and fate of a natural *Trichodesmium* bloom. We recognize that the enclosure and incubation of collected biomass in bottles and carboys may accelerate cellular processes compared to the natural lagoon setting. However, the published rates of *Trichodesmium* mortality from field studies (Rodier and Le Borgne, 2010) indicate that these can parallel our loss rates with natural bloom demise occurring 24–48 h after peak of biomass.

We focused initially on biotic factors that could impact the incubated *Trichodesmium* biomass. The low number of harpacticoid zooplankton specific to *Trichodesmium* (O’Neil and Roman, 1994; O’Neil, 1998) in the lagoon (Hunt et al., 2016) and especially those in the bottles (personal observation) refutes the possibility that grazing caused the massive mortality of *Trichodesmium* biomass in our experimental incubations.

Viruses have been increasingly invoked as key agents terminating phytoplankton blooms (Brussaard et al., 2005; Jacquet et al., 2002; Lehahn et al., 2014; Tarutani et al., 2000; Vardi et al., 2012). Infection by phages has been invoked as the mechanism of *Trichodesmium* bloom crashes, but it has yet to be unequivocally demonstrated (Hewson et al., 2004; Ohki, 1999); indeed, no specific *Trichodesmium* phage has been isolated or characterized to date (Brown et al., 2013). Here, total VLP abundance was highest at the time of sampling from the surface *Trichodesmium* bloom and at the start of the incubation ($\sim 8 \times 10^6 \text{ VLP mL}^{-1}$). It actually declined 2-fold in the first 8 h of incubation before increasing over the next 32 h (Fig. 4a). While our method of analysis cannot distinguish between phages infecting *Trichodesmium* from those infecting other marine bacteria, it argues against a massive, phage-induced lytic event of *Trichodesmium*. Such an event would have yielded a notable burst of VLP upon bloom crash, especially considering the high *Trichodesmium* biomass observed. The coincidence between the maximal abundance of VLP and highest *Trichodesmium* biomass is

counter to viruses serving as the mechanism of mortality in our incubation experiments. Nonetheless, virus infection itself may be a stimulant for community N₂ fixation perhaps by releasing key nutrients (i.e., P or Fe) upon lysis of surrounding microbes (Weitz and Wilhelm, 2012). Although we did not characterize them here, it is indeed possible that *Trichodesmium*-specific phages were present in our incubation experiments and they may have exerted additional physiological stress on resident populations, facilitating PCD induction. Virus infection has been shown to increase the cellular production of reactive oxygen species (Evans et al., 2006; Vardi et al., 2012), which in turn can stimulate PCD in algal cells (Berman-Frank et al., 2004; Bidle, 2015; Thamatrakoln et al., 2012). Viral attack can also directly trigger PCD as part of an antiviral defense system activated to limit virus production and prevent massive viral infection (Bidle and Falkowski, 2004; Bidle, 2015; Georgiou et al., 1998).

4.1.2 Stressors impacting mortality

Nutrient stress can be acute or chronic to which organisms may acclimate on different timescales. Thus, for example, the consistently low DIP concentrations measured in the lagoon during the 22 days preceding the *Trichodesmium* surface bloom probably enabled acclimation responses such as induction of APA and other P acquisition systems. *Trichodesmium* has the ability to obtain P via inorganic and organic sources, including methylphosphonate, ethylphosphonate, and 2-aminoethylphosphonate (Beversdorf et al., 2010; Dyhrman et al., 2006), and via a phosphite uptake system (PtxABC) that accesses P via the reduced inorganic compound phosphite (Martínez et al., 2012; Polyviou et al., 2015). Our metatranscriptomic data demonstrated upregulated expression of genes related to all three of these uptake systems (DIP, phosphonates, phosphites) 8 and 22 h after incubation began, accompanying biomass demise (Fig. 5a). This included one gene for phosphite uptake (*ptxA*) and several genes from the phosphonate uptake operon (*phnDCEEGHIJKLM*) (Hove-Jensen et al., 2014). Upregulated expression of *phnD*, *phnC*, *phnE*, *phnH*, *phnI*, *phnJ*, *phnK*, *phnL*, and *phnM* occurred as the *Trichodesmium* biomass crashed (Fig. 5a, Table S1), consistent with previous results demonstrating that *phnD* and *phnJ* expression levels increased during DIP depletion (Hove-Jensen et al., 2014). It is likely that, during bloom demise, the C-P lyase pathway of remaining living cells was induced when DIP sources were extremely low, while POP and DOP increased along with the decaying organic matter. The ability to use phosphonates or phosphites as a P source can provide a competitive advantage for phytoplankton and bacteria in P-depleted waters (Coleman and Chisholm, 2010; Martinez et al., 2010). Thus, it is puzzling why dying cells would upregulate *phn* genes or *phoA* transcripts after 22 h incubation (Fig. 5a). A more detailed temporal resolution of the metatranscriptomic analyses may elucidate the expression dynamics of these genes

and their regulating factors. Alternatively, in PCD-induced populations, a small percentage of cells remain viable and resistant as either cysts (Vardi et al., 1999) or hormogonia (Berman-Frank et al., 2004) that can serve as the inoculum for future blooms. It is plausible that the observed upregulation signal was attributable to these subpopulations.

The concentrations of dissolved and bioavailable Fe were not measured in the lagoon water during the experimental period as Fe is typically replete in the lagoon (Jacquet et al., 2006). However, even in Fe-replete environments such as the New Caledonian lagoon, dense patches of cyanobacterial or algal biomass can deplete available resources and cause limited microenvironments (Shaked, 2002). We obtained evidence for Fe stress using several proxy genes demonstrating that enhanced cellular Fe demand occurred during the bloom crash (Table S1). *Trichodesmium*'s strategies of obtaining and maintaining sufficient Fe involves genes such as *isiB*. *isiB* was highly expressed when biomass accumulated on the surface waters, indicative for higher Fe demand at this biomass load (Bar-Zeev et al., 2013; Chappell and Webb, 2010), yet expression declined significantly with the dying biomass. Transcripts for chlorophyll-binding, Fe-stress-induced protein A (*IsiA*) increased (albeit not significantly) 3-fold over 22 h of bloom demise (Fig. 5b, Table S1). In many cyanobacteria, *isiA* expression is stimulated under Fe stress (Laudenbach and Straus, 1988) and oxidative stress (Jeanjean et al., 2003) and functions to prevent high light-induced oxidative damage by increasing cyclic electron flow around the photosynthetic reaction center photosystem I (Havaux et al., 2005; Latifi et al., 2005; Michel and Pistorius, 2004). Dense surface blooms of *Trichodesmium* are exposed to high irradiance (on day 23 average photosynthetically active radiation was 3000 $\mu\text{mol photons m}^{-2} \text{s}^{-1}$). It is possible that high Fe demand combined with the oxidative stress of the high irradiance induced the higher expression of *isiA* (Fig. 5b). As cell density and associated self-shading of *Trichodesmium* filaments decreased during bloom crash, light-induced oxidative stress is likely the principal driver for elevated *isiA* expression.

The gene *idiA* is another environmental Fe stress biomarker that allows acquisition and transfer of Fe through the periplasm into the cytoplasm (Chappell and Webb, 2010). In our incubation, upregulated expression of *idiA* (an ABC Fe⁺³ transporter) was evident after 8 h. This is consistent with increasing Fe limitation, as *Trichodesmium* abundance (measured via 16S rRNA gene sequencing) was still high at *T*₆ (after 6 h of incubation) (replicate 1). These findings are consistent with proteomics analyses from depleted iron (0 μM Fe) *Trichodesmium* cultures which revealed an increase in *IdiA* protein expression (Snow et al., 2015). Lastly, our metatranscriptomic data highlighted a reduction in Fe storage and utilization, as the expression of Fe-rich ferritin-like DPS proteins (Castruita et al., 2006), encoded by *dpsA*, decreased ~ 5 -fold by the time that most of the biomass had crashed (*T*₂₂) (Fig. 5b, Table S1). *dpsA* was also downregu-

lated under Fe-replete conditions in *Synechococcus* (Mackey et al., 2015), but the downregulation observed here is more likely related to *Trichodesmium* cells dying and downregulating Fe-demanding processes such as photosynthesis and N₂ fixation.

4.1.3 Programmed cell death (PCD) and markers for increased export flux

The physiological and morphological evidence of PCD in *Trichodesmium* has been previously documented in both laboratory (Bar-Zeev et al., 2013; Berman-Frank et al., 2004) and environmental cultures collected from surface waters around New Caledonia (Berman-Frank et al., 2004). Here, we confirmed characteristic features of autocatalytic PCD in *Trichodesmium* such as increased caspase-specific activity (Fig. 6a), globally enhanced metacaspase expression (Fig. 6b), and decreased expression of gas vesicle maintenance (Fig. 7). Metatranscriptomic snapshots interrogating expression changes in all of the annotated *Trichodesmium* metacaspases (Fig. 6b) generally portrayed upregulated expression concomitant with biomass decline. Our results are consistent with previous observations that Fe-depleted PCD-induced laboratory cultures of *Trichodesmium* IMS101 had higher expression levels of TeMC1 and TeMC9 compared to healthy Fe-replete cultures (Bar-Zeev et al., 2013; Berman-Frank et al., 2004). To our knowledge, this is the first study examining expression levels of metacaspases in environmental *Trichodesmium* samples during a natural bloom. Eleven of the 12 metacaspases in *Trichodesmium* were expressed in all three metatranscriptomes from the surface bloom. To date, no specific function has been determined for these metacaspases in *Trichodesmium* other than their association with cellular stress and death. Efforts are underway to elucidate the specific cellular functions, regulation, and protein interactions of these *Trichodesmium* metacaspases (Bar-Zeev et al., 2013; Pfreundt et al., 2014; D. Spungin, personal communication, 2016).

In cultures and isolated natural populations of *Trichodesmium*, high caspase-like specific activity is correlated with the initial induction stages of PCD with activity declining as the biomass crashes (Bar-Zeev et al., 2013; Berman-Frank et al., 2004, 2007). Here, caspase-like activity increased with the crashing populations of *Trichodesmium* (Fig. 6a). Notably, maximal caspase activities were recorded at T_{22} , after which most *Trichodesmium* biomass had collapsed. The high protein-normalized caspase-specific activity may be a result of a very stressed and dying subpopulation of *Trichodesmium* that had not yet succumbed to PCD (Berman-Frank et al., 2004). Alternatively, the high caspase-like activity may be attributed to the large population of *Alteromonas* bacteria that were associated with the remaining detrital *Trichodesmium* biomass. However, currently, we are unaware of any publications demonstrating high cellular caspase-specific activity in clades of γ -Proteobacteria.

Gas vesicles are internal structures essential for maintaining buoyancy of *Trichodesmium* populations in the upper surface waters enabling them to vertically migrate and respond to light and nutrient requirements (Capone et al., 1997; Walsby, 1978). Mortality via PCD causes a decline in the number and size of cellular gas vesicles in *Trichodesmium* (Berman-Frank et al., 2004) and results in an enhanced vertical flux of trichomes and colonies to depth (Bar-Zeev et al., 2013). Our metatranscriptomic data supported the subcellular divestment from gas vesicle production during bloom decline, as the expression of vesicle-related genes was downregulated (Fig. 7). In parallel, TEP production and concentration increased to $> 800 \mu\text{g GX L}^{-1}$, a 2-fold increase from pre-bloom periods (Figs. 1d and 4c). When nutrient uptake is limited, but CO₂ and light are sufficient, uncoupling occurs between photosynthesis and growth (Berman-Frank and Dubinsky, 1999), leading to increased production of excess polysaccharides (such as TEP) and corresponding with high TEP found in bloom decline phases rather than during the increase in population density (Engel, 2000; Smetacek, 1985). In earlier studies we demonstrated that PCD-induced demise in *Trichodesmium* is characterized by an increase in excreted TEP (Berman-Frank et al., 2007) and enhanced sinking of particulate organic matter (Bar-Zeev et al., 2013). TEP may be positively buoyant (Azetsu-Scott and Passow, 2004), yet their stickiness causes aggregation and clumping of cells and detritus, ultimately enhancing sinking rates of large aggregates, including dying *Trichodesmium* (Bar-Zeev et al., 2013).

4.1.4 Changes in microbial community with *Trichodesmium* decline

In the incubations, other diazotrophic populations succeeded the declining *Trichodesmium* biomass as indicated by increasing N₂-fixation rates, POC, and PON (Fig. 4b). In experiment 2, based on qPCR of targeted diazotrophic phylogenotypes, the diazotroph community composition shifted from being dominated by *Trichodesmium* spp. and unicellular groups UCYN-A1, UCYN-A2, and UCYN-B (T_0) to one dominated by diatom–diazotroph associations Het-1 and Het-2 (T_{72}) (Bonnet et al., 2016b; K. Turk-Kubo, personal communication, 2016). In experiment 1 heterotrophic bacteria thrived and increased in abundance as the *Trichodesmium* biomass crashed (Fig. 3).

Trichodesmium colonies host a wide diversity of microorganisms, including specific epibionts, viruses, bacteria, eukaryotic microorganisms, and metazoans (Hewson et al., 2009; Hmelo et al., 2012; Ohki, 1999; Paerl et al., 1989; Sheridan et al., 2002; Siddiqui et al., 1992; Zehr, 1995). Associated epibiont bacterial abundance in dilute and exponentially growing laboratory cultures of *Trichodesmium* is relatively limited (Spungin et al., 2014) compared to bloom conditions (Hewson et al., 2009; Hmelo et al., 2012). Proliferation of *Alteromonas* and other γ -Proteobacteria during

biomass collapse (Fig. 3) confirms their reputation as opportunistic microorganisms (Allers et al., 2008; Hewson et al., 2009; Frydenborg et al., 2014; Pichon et al., 2013). Such organisms can thrive on the influx of organic nutrient sources from the decaying *Trichodesmium* as we observed (Fig. 3). Furthermore, the increase in organic matter including TEP produced by the stressed *Trichodesmium* (Figs. 1d and 4c) probably stimulated growth of these copiotrophs. Moreover, as the *Trichodesmium* biomass declined in the carboys, the high concentrations of NH_4^+ ($> 5000 \text{ nmol L}^{-1}$) (Fig. 4b) sustained both autotrophic and heterotrophic organisms (Berthelot et al., 2015; Bonnet et al., 2016b, c). Thus, the increase in volumetric N_2 fixation and PON that was measured in the incubation bottles right after the *Trichodesmium* crash in experiment 2 (Fig. 4b) probably reflects both the enhanced activity of other diazotrophs (see above and Bonnet et al., 2016b) and the resistant residual *Trichodesmium* trichomes (Berman-Frank et al., 2004) with increased cell-specific N_2 fixation. This scenario is consistent with the hypothesis that PCD induction and death of a fraction of the population confers favorable conditions for survival and growth of individual cells (Bidle and Falkowski, 2004; Bidle, 2015).

4.2 Implications for the lagoon system and export flux

Phytoplankton blooms and their dense surface accumulations occur under favorable physical properties of the upper ocean (e.g., temperature, mixed-layer depth, stratification) and specifically when division rates exceed loss rates derived from grazing, viral attack, and sinking or export from the mixed layer to depth (Behrenfeld, 2014). Although physical drivers such as turbulence and mixing may scatter and dilute these dense accumulations, the rapid disappearance of biomass in large sea-surface *Trichodesmium* blooms (within 1–2 days in the lagoon waters) (Rodier and Le Bourne, 2010) suggests loss of biomass by other mechanisms. The lack of *Trichodesmium* developing within the VAHINE mesocosms and the spatial–temporal variability in the surface bloom in the lagoon prohibited in situ sampling of the same biomass for several days and prevented conclusions regarding in situ mortality rates and export flux. Furthermore, within these dense surface populations, as well as in the microcosm and carboy experiments, Fe availability was probably extremely limited due to high cellular demand and competition (Shaked, 2002). PCD induced by Fe-depletion experiments with laboratory cultures and natural populations results in rapid biomass demise, typically beginning after 24 h, with $> 90\%$ of the biomass crashing 3 to 5 days after induction (Bar-Zeev et al., 2013; Berman-Frank et al., 2004; Berman-Frank et al., 2007). In similar experiments with P depletion, *Trichodesmium* biomass did not crash rapidly. Rather, limitation induced colony formation and elongation of trichomes (Spungin et al., 2014) and the cultures could be sustained for another couple of weeks before biomass declined significantly (unpublished data). The responses we quantified from

the dying *Trichodesmium* in the carboys and bottles (Figs. 3–7) were similar to those obtained from controlled laboratory experiments where P and Fe stress was validated individually. However, the rapid response here probably reflects an exacerbated reaction due to the simultaneous combination of different stressors and the presence of biotic components that can compete for and utilize the organic resources (carbon, nitrogen, phosphorus) generated by the dying *Trichodesmium*. In the lagoon, production of TEP by stressed biomass combined with the degradation of gas vesicles and enhanced aggregation will cause such surface accumulations or blooms to collapse, leading to rapid vertical export of newly fixed nitrogen and carbon in the ocean.

5 Conclusions and implications

We demonstrate that the rapid demise of a *Trichodesmium* surface bloom in New Caledonia, with the disappearance of $> 90\%$ of the biomass within 24 h in 4.5 L bottle incubations, displayed cellular responses to P and Fe stress and was mediated by a suite of PCD genes. Virus infection and lysis did not appear to directly cause the massive biomass decline. Although virus infection may have modulated the cellular and genetic responses to enhance PCD-driven loss processes, quorum sensing among epibionts (Hmelo et al., 2012; Van Mooy et al., 2012), allelopathic interactions, and the production of toxins by *Trichodesmium* (Guo and Tester, 1994; Kerbrat et al., 2010) are additional factors that could be important for a concerted response of the *Trichodesmium* population, but we did not examine them here. Collectively, they would facilitate rapid collapse and loss of *Trichodesmium* populations and possibly lead to enhanced vertical fluxes and export production, as previously demonstrated in PCD-induced laboratory cultures of *Trichodesmium* (Bar-Zeev et al., 2013). We posit that PCD-induced demise, in response to concurrent cellular stressors and facilitated by concerted gene regulation, is typical in natural *Trichodesmium* blooms and leads to a high export production rather than regeneration and recycling of biomass in the upper photic layers.

6 Data availability

The raw transcriptomic data for T_0 , T_8 , and T_{22} are available from NCBI short read archive under the bioproject accession number PRJNA304389, biosample accessions SAMN05207415, SAMN05207416, and SAMN05207417.

The Supplement related to this article is available online at doi:10.5194/bg-13-4187-2016-supplement.

Author contributions. Ilana Berman-Frank, Dina Spungin, and Sophie Bonnet conceived and planned the study. Dina Spungin, Ulrike Pfreundt, Hugo Berthelot, Sophie Bonnet, Wolfgang R. Hess, Kay D. Bidle, and Ilana Berman-Frank participated in the experimental sampling. Dina Spungin, Ulrike Pfreundt, Wolfgang R. Hess, Hugo Berthelot, Frank Natale, Dina AlRoumi, Kay D. Bidle, and Ilana Berman-Frank analyzed the samples and resulting data. Ilana Berman-Frank and Dina Spungin wrote the manuscript with further contributions to the manuscript by Ulrike Pfreundt, Wolfgang R. Hess, Sophie Bonnet, and Kay D. Bidle.

Acknowledgements. Funding was obtained for Ilana Berman-Frank through a collaborative grant from MOST Israel and the High Council for Science and Technology (HCST), France, and a United States–Israel Binational Science Foundation (BSF) grant (no. 2008048) to Ilana Berman-Frank and Kay D. Bidle. This research was partially funded by the Gordon and Betty Moore Foundation through grant GBMF3789 to KDB. The participation of Ilana Berman-Frank, Dina Spungin, Ulrike Pfreundt, and Wolfgang R. Hess in the VAHINE experiment was supported by the German-Israeli Research Foundation (GIF), project number 1133-13.8/2011 to Ilana Berman-Frank and Wolfgang R. Hess, and the metatranscriptome analysis by the EU project MaCuMBA (Marine Microorganisms: Cultivation Methods for Improving their Biotechnological Applications; grant agreement no. 311975) to Wolfgang R. Hess. Funding for the VAHINE experimental project was provided by the Agence Nationale de la Recherche (ANR starting grant VAHINE ANR-13-JS06-0002), INSU-LEFE-CYBER program, GOPS, IRD, and MIO. The authors thank the captain and crew of the R/V *Alis*, the SEOH divers service from the IRD research center of Noumea (E. Folcher, B. Bourgeois, and A. Renaud) and from the Observatoire Océanologique de Villefranche-sur-mer (OOV, J. M. Grisoni), and the IRD research center of Noumea for their helpful technical support. Thanks especially to E. Rahav for his assistance throughout the New Caledonia experiment and to H. Elifantz for assistance with the 16S sequencing and data analysis. This work is in partial fulfillment of the requirements for a PhD thesis for D. Spungin at Bar-Ilan University. We thank the three reviewers, whose comments helped improve the manuscript substantially.

Edited by: D. G. Capone

Reviewed by: three anonymous referees

References

- Allers, E., Niesner, C., Wild, C., and Pernthaler, J.: Microbes enriched in seawater after addition of coral mucus, *Appl. Environ. Microbiol.*, 74, 3274–3278, 2008.
- Anders, S., Pyl, P. T., and Huber, W.: HTSeq—A Python framework to work with high-throughput sequencing data, *Bioinformatics*, 31, 166–169, 2015.
- Asplund-Samuelsson, J., Bergman, B., and Larsson, J.: Prokaryotic caspase homologs: phylogenetic patterns and functional characteristics reveal considerable diversity, *PLOS One*, 7, e49888, doi:10.1371/journal.pone.0049888, 2012.
- Asplund-Samuelsson, J.: The art of destruction: revealing the proteolytic capacity of bacterial caspase homologs, *Mol. Microbiol.*, 98, 1–6, 2015.
- Azetsu-Scott, K. and Passow, U.: Ascending marine particles: Significance of transparent exopolymer particles (TEP) in the upper ocean, *Limnol. Oceanogr.*, 49, 741–748, 2004.
- Bar-Zeev, E., Avishay, I., Bidle, K. D., and Berman-Frank, I.: Programmed cell death in the marine cyanobacterium *Trichodesmium* mediates carbon and nitrogen export, *The ISME Journal*, 7, 2340–2348, 2013.
- Behrenfeld, M. J.: Climate-mediated dance of the plankton, *Nature Climate Change*, 4, 880–887, 2014.
- Bergman, B., Sandh, G., Lin, S., Larsson, J., and Carpenter, E. J.: *Trichodesmium* — a widespread marine cyanobacterium with unusual nitrogen fixation properties, *FEMS Microbiol. Rev.*, 37, 286–302, 10.1111/j.1574-6976.2012.00352.x., 2012.
- Berman-Frank, I. and Dubinsky, Z.: Balanced growth in aquatic plants: Myth or reality? Phytoplankton use the imbalance between carbon assimilation and biomass production to their strategic advantage, *Bioscience*, 49, 29–37, 1999.
- Berman-Frank, I., Cullen, J. T., Shaked, Y., Sherrell, R. M., and Falkowski, P. G.: Iron availability, cellular iron quotas, and nitrogen fixation in *Trichodesmium*, *Limnol. Oceanogr.*, 46, 1249–1260, 2001.
- Berman-Frank, I., Bidle, K., Haramaty, L., and Falkowski, P. G.: The demise of the marine cyanobacterium, *Trichodesmium* spp., via an autocatalyzed cell death pathway, *Limnol. Oceanogr.*, 49, 997–1005, 2004.
- Berman-Frank, I., Rosenberg, G., Levitan, O., Haramaty, L., and Mari, X.: Coupling between autocatalytic cell death and transparent exopolymeric particle production in the marine cyanobacterium *Trichodesmium*, *Environ. Microbiol.*, 9, 1415–1422, 2007.
- Berthelot, H., Moutin, T., L’Helguen, S., Leblanc, K., Hélias, S., Grosso, O., Leblond, N., Charrière, B., and Bonnet, S.: Dinitrogen fixation and dissolved organic nitrogen fueled primary production and particulate export during the VAHINE mesocosm experiment (New Caledonia lagoon), *Biogeosciences*, 12, 4099–4112, doi:10.5194/bg-12-4099-2015, 2015.
- Beversdorf, L., White, A., Björkman, K., Letelier, R., and Karl, D.: Phosphonate metabolism by *Trichodesmium* IMS101 and the production of greenhouse gases, *Limnol. Oceanogr.*, 55, 1768–1778, 2010.
- Bidle, K. D.: The molecular ecophysiology of programmed cell death in marine phytoplankton, *Ann. Rev. Mar. Sci.*, 7, 341–375, 2015.
- Bidle, K. D. and Falkowski, P. G.: Cell death in planktonic, photosynthetic microorganisms, *Nat. Rev. Microbiol.*, 2, 643–655, 2004.
- Bonnet, S., Moutin, T., Rodier, M., Grisoni, J.-M., Louis, F., Folcher, E., Bourgeois, B., Boré, J.-M., and Renaud, A.: Introduction to the project VAHINE: Variability of vertical and trophic transfer of diazotroph derived N in the south west Pacific, *Biogeosciences*, 13, 2803–2814, doi:10.5194/bg-13-2803-2016, 2016a.
- Bonnet, S., Berthelot, H., Turk-Kubo, K., Cornet-Barthaux, V., Fawcett, S., Berman-Frank, I., Barani, A., Dekeazemacker, J., Benavides, M., Charrière, B., and Capone, D.: *Trichodesmium*

- blooms support diatom growth in the Southwest Pacific Ocean, *Limnol. Oceanogr.*, in press, doi:10.1002/lno.10300, 2016b.
- Bonnet, S., Berthelot, H., Turk-Kubo, K., Fawcett, S., Rahav, E., L'Helguen, S., and Berman-Frank, I.: Dynamics of N₂ fixation and fate of diazotroph-derived nitrogen in a low-nutrient, low-chlorophyll ecosystem: results from the VAHINE mesocosm experiment (New Caledonia), *Biogeosciences*, 13, 2653–2673, doi:10.5194/bg-13-2653-2016, 2016c.
- Brown, J. M., LaBarre, B. A., and Hewson, I.: Characterization of *Trichodesmium*-associated viral communities in the eastern Gulf of Mexico, *FEMS Microbiol. Ecol.*, 84, 603–613, 2013.
- Brussaard, C. R. D.: Optimization of procedures for counting viruses by flow cytometry, *App. Environ. Microbiol.*, 70, 1506–1513, 2003.
- Brussaard, C. P. D., Mari, X., Van Bleijswijk, J. D. L., and Veldhuis, M. J. W.: A mesocosm study of *Phaeocystis globosa* (Prymnesiophyceae) population dynamics – II. Significance for the microbial community, *Harmful Algae*, 4, 875–893, 2005.
- Capone, D. G. and Carpenter, E. J.: Nitrogen fixation in the marine environment, *Science*, 217, 1140–1142, 1982.
- Capone, D., Burns, J., Montoya, J., Michaels, A., Subramaniam, A., and Carpenter, E.: New nitrogen input to the tropical North Atlantic Ocean by nitrogen fixation by the cyanobacterium, *Trichodesmium* spp., *Global Biogeochem. Cy.*, 19, GB2024, doi:10.1029/2004GB002331, 2004.
- Capone, D. G., Zehr, J. P., Paerl, H. W., Bergman, B., and Carpenter, E. J.: *Trichodesmium*, a globally significant marine cyanobacterium, *Science*, 276, 1221–1229, 1997.
- Capone, D. G., Subramaniam, A., Montoya, J. P., Voss, M., Humberg, C., Johansen, A. M., Siefert, R. L., and Carpenter, E. J.: An extensive bloom of the N₂-fixing cyanobacterium *Trichodesmium erythraeum* in the central Arabian Sea, *Mar. Ecol. Prog. Ser.*, 172, 281–292, 1998.
- Castruita, M., Saito, M., Schottel, P., Elmegreen, L., Myneni, S., Stiefel, E., and Morel, F. M.: Overexpression and characterization of an iron storage and DNA-binding Dps protein from *Trichodesmium erythraeum*, *Appl. Environ. Microbiol.*, 72, 2918–2924, 2006.
- Chappell, P. D. and Webb, E. A.: A molecular assessment of the iron stress response in the two phylogenetic clades of *Trichodesmium*, *Environ. Microbiol.*, 12, 13–27, 2010.
- Coleman, M. L. and Chisholm, S. W.: Ecosystem-specific selection pressures revealed through comparative population genomics, *P. Natl. Acad. Sci.*, 107, 18634–18639, 2010.
- Dandonneau, Y. and Gohin, F.: Meridional and seasonal variations of the sea surface chlorophyll concentration in the southwestern tropical Pacific (14 to 32° S, 160 to 175° E), *Deep-Sea Res. Pt. A*, 31, 1377–1393, 1984.
- Dowd, S. E., Callaway, T. R., Wolcott, R. D., Sun, Y., McKeehan, T., Hagevoort, R. G., and Edrington, T. S.: Evaluation of the bacterial diversity in the feces of cattle using 16S rDNA bacterial tag-encoded FLX amplicon pyrosequencing (bTEFAP), *BMC Microbiology*, 8, 125, doi:10.1186/1471-2180-8-125, 2008.
- Dupouy, C., Benielli-Gary, D., Neveux, J., Dandonneau, Y., and Westberry, T. K.: An algorithm for detecting *Trichodesmium* surface blooms in the South Western Tropical Pacific, *Biogeosciences*, 8, 3631–3647, 10.5194/bg-8-3631-2011, 2011.
- Dyhrman, S. T., Chappell, P. D., Haley, S. T., Moffett, J. W., Orchard, E. D., Waterbury, J. B., and Webb, E. A.: Phosphonate utilization by the globally important marine diazotroph *Trichodesmium*, *Nature*, 439, 68–71, 2006.
- Edgar, R. C.: UPARSE: highly accurate OTU sequences from microbial amplicon reads, *Nature Methods*, 10, 996–998, 2013.
- Engel, A.: The role of transparent exopolymer particles (TEP) in the increase in apparent particle stickiness (alpha) during the decline of a diatom bloom, *J. Plankt. Res.*, 22, 485–497, 2000.
- Evans, C., Malin, G., Mills, G. P., and Wilson, W. H.: Viral infection of *Emiliania huxleyi* (prymnesiophyceae) leads to elevated production of reactive oxygen species, *J. Phycol.*, 42, 1040–1047, 2006.
- Frydenborg, B. R., Krediet, C. J., Teplitski, M., and Ritchie, K. B.: Temperature-dependent inhibition of opportunistic vibrio pathogens by native coral commensal bacteria, *Microb. Ecol.*, 67, 392–401, 2014.
- Georgiou, T., Yu, Y.-T., Ekunwe, S., Buttner, M., Zuurmond, A.-M., Kraal, B., Kleantous, C., and Snyder, L.: Specific peptide-activated proteolytic cleavage of *Escherichia coli* elongation factor Tu, *P. Natl. Acad. Sci.*, 95, 2891–2895, 1998.
- Guo, C. and Tester, P. A.: Toxic effect of the bloom-forming *Trichodesmium* sp. (Cyanophyta) to the copepod *Acartia tonsa*, *Natural Toxins*, 2, 222–227, 1994.
- Hamady, M., Walker, J. J., Harris, J. K., Gold, N. J., and Knight, R.: Error-correcting barcoded primers for pyrosequencing hundreds of samples in multiplex, *Nature Methods*, 5, 235–237, 2008.
- Havaux, M., Guedeny, G., Hagemann, M., Yermenko, N., Matthijs, H. C., and Jeanjean, R.: The chlorophyll-binding protein IsiA is inducible by high light and protects the cyanobacterium *Synechocystis* PCC6803 from photooxidative stress, *FEBS Letters*, 579, 2289–2293, 2005.
- Herbland, A., Le Bouteiller, A., and Raimbault, P.: Size structure of phytoplankton biomass in the equatorial Atlantic Ocean, *Deep-Sea Res. Pt. A*, 32, 819–836, 1985.
- Hewson, I., Govil, S. R., Capone, D. G., Carpenter, E. J., and Fuhrman, J. A.: Evidence of *Trichodesmium* viral lysis and potential significance for biogeochemical cycling in the oligotrophic ocean, *Aquat. Microb. Ecol.*, 36, 1–8, 2004.
- Hewson, I., Poretsky, R. S., Dyhrman, S. T., Zielinski, B., White, A. E., Tripp, H. J., Montoya, J. P., and Zehr, J. P.: Microbial community gene expression within colonies of the diazotroph, *Trichodesmium*, from the Southwest Pacific Ocean, *ISME Journal*, 3, 1286–1300, 2009.
- Hmelo, L. R., Van Mooy, B. A. S., and Mincer, T. J.: Characterization of bacterial epibionts on the cyanobacterium *Trichodesmium*, *Aquat. Microb. Ecol.*, 67, 1-U119, doi:10.3354/ame01571, 2012.
- Holmes, R. M., Aminot, A., K  rouel, R., Hooker, B. A., and Peterson, B. J.: A simple and precise method for measuring ammonium in marine and freshwater ecosystems, *Can. J. Fish. Aquat. Sci.*, 56, 1801–1808, 1999.
- Hove-Jensen, B., Zechel, D. L., and Jochimsen, B.: Utilization of Glyphosate as Phosphate Source: Biochemistry and Genetics of Bacterial Carbon-Phosphorus Lyase, *Microbiol. Mol. Biol. Rev.*, 78, 176–197, 2014.
- Hunt, B. P. V., Bonnet, S., Berthelot, H., Conroy, B. J., Foster, R. A., and Pagano, M.: Contribution and pathways of diazotroph-derived nitrogen to zooplankton during the VAHINE mesocosm experiment in the oligotrophic New Caledonia lagoon, *Biogeosciences*, 13, 3131–3145, doi:10.5194/bg-13-3131-2016, 2016.

- Ivars-Martinez, E., Martin-Cuadrado, A.-B., D'Auria, G., Mira, A., Ferriera, S., Johnson, J., Friedman, R., and Rodriguez-Valera, F.: Comparative genomics of two ecotypes of the marine planktonic copiotroph *Alteromonas macleodii* suggests alternative lifestyles associated with different kinds of particulate organic matter, *The ISME Journal*, 2, 1194–1212, 2008.
- Jacquet, S., Heldal, M., Iglesias-Rodriguez, D., Larsen, A., Wilson, W., and Bratbak, G.: Flow cytometric analysis of an *Emiliana huxleyi* bloom terminated by viral infection, *Aquat. Microb. Ecol.*, 27, 111–124, 2002.
- Jacquet, S., Delesalle, B., Torrétou, J.-P., and Blanchot, J.: Response of phytoplankton communities to increased anthropogenic influences (southwestern lagoon, New Caledonia), *Mar. Ecol. Prog. Ser.*, 320, 65–78, 2006.
- Jeanjean, R., Zuther, E., Yeremenko, N., Havaux, M., Matthijs, H. C., and Hagemann, M.: A photosystem 1 *psaFJ*-null mutant of the cyanobacterium *Synechocystis* PCC 6803 expresses the *isiAB* operon under iron replete conditions, *FEBS Letters*, 549, 52–56, 2003.
- Kerbrat, A.-S., Darius, H. T., Pauillac, S., Chinain, M., and Laurent, D.: Detection of ciguatoxin-like and paralyzing toxins in *Trichodesmium* spp. from New Caledonia lagoon, *Mar. Pollut. Bull.*, 61, 360–366, 2010.
- Kopylova, E., Noé, L., and Touzet, H.: SortMeRNA: fast and accurate filtering of ribosomal RNAs in metatranscriptomic data, *Bioinformatics*, 28, 3211–3217, 2012.
- Langmead, B. and Salzberg, S. L.: Fast gapped-read alignment with Bowtie 2, *Nat. Methods*, 9, 357–359, 2012.
- Latifi, A., Jeanjean, R., Lemeille, S., Havaux, M., and Zhang, C.-C.: Iron starvation leads to oxidative stress in *Anabaena* sp. strain PCC 7120, *J. Bacteriol.*, 187, 6596–6598, 2005.
- Laudenbach, D. E. and Straus, N. A.: Characterization of a cyanobacterial iron stress-induced gene similar to *psbC*, *J. Bacteriol.*, 170, 5018–5026, 1988.
- Leblanc, K., Cornet, V., Caffin, M., Rodier, M., Desnues, A., Berthelot, H., Turk-Kubo, K., and Heliou, J.: Phytoplankton community structure in the VAHINE MESOCOSM experiment, *Biogeosciences Discuss.*, doi:10.5194/bg-2015-605, in review, 2016.
- Lehahn, Y., Koren, I., Schatz, D., Frada, M., Sheyn, U., Boss, E., Efrati, S., Rudich, Y., Trainic, M., and Sharoni, S.: Decoupling physical from biological processes to assess the impact of viruses on a mesoscale algal bloom, *Curr. Biol.*, 24, 2041–2046, 2014.
- Luo, Y.-W., Doney, S. C., Anderson, L. A., Benavides, M., Berman-Frank, I., Bode, A., Bonnet, S., Boström, K. H., Böttjer, D., Capone, D. G., Carpenter, E. J., Chen, Y. L., Church, M. J., Dore, J. E., Falcón, L. I., Fernández, A., Foster, R. A., Furuya, K., Gómez, F., Gundersen, K., Hynes, A. M., Karl, D. M., Kitajima, S., Langlois, R. J., LaRoche, J., Letelier, R. M., Marañón, E., McGillicuddy Jr., D. J., Moisaner, P. H., Moore, C. M., Mourino-Carballido, B., Mulholland, M. R., Needoba, J. A., Orcutt, K. M., Poulton, A. J., Rahav, E., Raimbault, P., Rees, A. P., Riemann, L., Shiozaki, T., Subramaniam, A., Tyrrell, T., Turk-Kubo, K. A., Varela, M., Villareal, T. A., Webb, E. A., White, A. E., Wu, J., and Zehr, J. P.: Database of diazotrophs in global ocean: abundance, biomass and nitrogen fixation rates, *Earth Syst. Sci. Data*, 4, 47–73, doi:10.5194/essd-4-47-2012, 2012.
- Mackey, K. R., Post, A. F., McIlvin, M. R., Cutter, G. A., John, S. G., and Saito, M. A.: Divergent responses of Atlantic coastal and oceanic *Synechococcus* to iron limitation, *P. Natl. Acad. Sci.*, 112, 9944–9949, 2015.
- Martin, M.: Cutadapt removes adapter sequences from high-throughput sequencing reads, *EMBnet Journal*, 17, 10–12, 2011.
- Martínez, A., Tyson, G. W., and DeLong, E. F.: Widespread known and novel phosphonate utilization pathways in marine bacteria revealed by functional screening and metagenomic analyses, *Environ. Microbiol.*, 12, 222–238, 2010.
- Martínez, A., Osburne, M. S., Sharma, A. K., DeLong, E. F., and Chisholm, S. W.: Phosphite utilization by the marine picocyanobacterium *Prochlorococcus* MIT9301, *Environ. Microbiol.*, 14, 1363–1377, 2012.
- Massana, R., Murray, A. E., Preston, C. M., and DeLong, E. F.: Vertical distribution and phylogenetic characterization of marine planktonic Archaea in the Santa Barbara Channel, *Appl. Environ. Microbiol.*, 63, 50–56, 1997.
- Michel, K. P. and Pistorius, E. K.: Adaptation of the photosynthetic electron transport chain in cyanobacteria to iron deficiency: the function of *IdiA* and *IsiA*, *Physiol. Plantarum*, 120, 36–50, 2004.
- Mohr, W., Großkopf, T., Wallace, D. W. R., and LaRoche, J.: Methodological underestimation of oceanic nitrogen fixation rates, *PLOS One*, 5, e12583, doi:10.1371/journal.pone.0012583, 2010.
- Montoya, J. P., Voss, M., Kahler, P., and Capone, D. G.: A simple, high-precision, high-sensitivity tracer assay for N₂ fixation, *Appl. Environ. Microbiol.*, 62, 986–993, 1996.
- Mulholland, M. R.: The fate of nitrogen fixed by diazotrophs in the ocean, *Biogeosciences*, 4, 37–51, doi:10.5194/bg-4-37-2007, 2007
- O'Neil, J. M.: The colonial cyanobacterium *Trichodesmium* as a physical and nutritional substrate for the harpacticoid copepod *Macrosetella gracilis*, *J. Plankt. Res.*, 20, 43–59, 1998.
- O'Neil, J. M. and Roman, M. R.: Ingestion of the Cyanobacterium *Trichodesmium* spp. by Pelagic Harpacticoid Copepods *Macrosetella*, *Miracia* and *Oculostella*, *Hydrobiologia*, 293, 235–240, 1994.
- Ohki, K.: A possible role of temperate phage in the regulation of *Trichodesmium* biomass, *Bulletin de l'institute oceanographique*, Monaco, 19, 287–291, 1999.
- Orchard, E., Webb, E., and Dyrhman, S.: Characterization of phosphorus-regulated genes in *Trichodesmium* spp., *The Biol. Bull.*, 205, 230–231, 2003.
- Paerl, H. W., Priscu, J. C., and Brawner, D. L.: Immunochemical localization of nitrogenase in marine *Trichodesmium* aggregates: Relationship to N₂ fixation potential, *Appl. Environ. Microbiol.*, 55, 2965–2975, 1989.
- Passow, U. and Alldredge, A. L.: A dye binding assay for the spectrophotometric measurement of transparent exopolymer particles (TEP), *Limnol. Oceanogr.*, 40, 1326–1335, 1995.
- Pfreundt, U., Kopf, M., Belkin, N., Berman-Frank, I., and Hess, W. R.: The primary transcriptome of the marine diazotroph *Trichodesmium erythraeum* IMS101, *Scientific Reports*, 4, 2014.
- Pfreundt, U., Van Wambeke, F., Caffin, M., Bonnet, S., and Hess, W. R.: Succession within the prokaryotic communities during the VAHINE mesocosms experiment in the New Caledonia lagoon, *Biogeosciences*, 13, 2319–2337, doi:10.5194/bg-13-2319-2016, 2016.
- Pichon, D., Cudennec, B., Huchette, S., Djediat, C., Renault, T., Paillard, C., and Auzoux-Bordenave, S.: Characterization of

- abalone *Haliotis tuberculata*–*Vibrio harveyi* interactions in gill primary cultures, *Cytotechnology*, 65, 759–772, 2013.
- Pinto, F. L., Thapper, A., Sontheim, W., and Lindblad, P.: Analysis of current and alternative phenol based RNA extraction methodologies for cyanobacteria, *BMC Mol. Biol.*, 10, doi:10.1186/1471-2199-10-79, 2009.
- Polyviou, D., Hitchcock, A., Baylay, A. J., Moore, C. M., and Bibby, T. S.: Phosphite utilization by the globally important marine diazotroph *Trichodesmium*, *Environ. Microbiol. Reports*, 7, 824–830, 2015.
- Pujo-Pay, M. and Raimbault, P.: Improvement of the wet-oxidation procedure for simultaneous determination of particulate organic nitrogen and phosphorus collected on filters, *Mar. Ecol.-Prog. Ser.*, 105, 203–207, 1994.
- Quast, C., Pruesse, E., Yilmaz, P., Gerken, J., Schweer, T., Yarza, P., Peplies, J., and Glöckner, F. O.: The SILVA ribosomal RNA gene database project: improved data processing and web-based tools, *Nucleic Acids Res.*, 41, D590–D596, 2013.
- Rahav, E., Herut, B., Levi, A., Mulholland, M. R., and Berman-Frank, I.: Springtime contribution of dinitrogen fixation to primary production across the Mediterranean Sea, *Ocean Sci.*, 9, 489–498, doi:10.5194/os-9-489-2013, 2013.
- Rodier, M. and Le Borgne, R.: Population dynamics and environmental conditions affecting *Trichodesmium* spp. (filamentous cyanobacteria) blooms in the south-west lagoon of New Caledonia, *J. Exp. Mar. Biol. Ecol.*, 358, 20–32, 2008.
- Rodier, M. and Le Borgne, R.: Population and trophic dynamics of *Trichodesmium thiebautii* in the SE lagoon of New Caledonia. Comparison with *T. erythraeum* in the SW lagoon, *Mar. Pollut. Bull.*, 61, 349–359, 2010.
- Shaked, Y.: Iron redox dynamics and biogeochemical cycling in the epilimnion of Lake Kinneret, PhD thesis, Hebrew University of Jerusalem, 2002.
- Sheridan, C. C., Steinberg, D. K., and Kling, G. W.: The microbial and metazoan community associated with colonies of *Trichodesmium* spp.: a quantitative survey, *J. Plankt. Res.*, 24, 913–922, 2002.
- Siddiqui, P. J., Bergman, B., Bjorkman, P. O., and Carpenter, E. J.: Ultrastructural and chemical assessment of poly-beta-hydroxybutyric acid in the marine cyanobacterium *Trichodesmium thiebautii*, *FEMS Microbiol. Lett.*, 73, 143–148, 1992.
- Smetacek, V.: Role of sinking in diatom life-history cycles: ecological, evolutionary and geological significance, *Mar. Biol.*, 84, 239–251, 1985.
- Snow, J. T., Polyviou, D., Skipp, P., Christmas, N. A. M., Hitchcock, A., Geider, R., Moore, C. M., and Bibby, T. S.: Quantifying Integrated Proteomic Responses to Iron Stress in the Globally Important Marine Diazotroph *Trichodesmium*, *PLOS One*, 10, e0142626, 10.1371/journal.pone.0142626, 2015.
- Spungin, D., Berman-Frank, I., and Levitan, O.: *Trichodesmium*'s strategies to alleviate phosphorus limitation in the future acidified oceans, *Environ. Microbiol.*, 16, 1935–1947, 2014.
- Strickland, J. D. H. and Parsons, T. R.: A Practical Handbook of Seawater Analysis, Fisheries Research Board of Canada, Ottawa, 1972.
- Tandeau de Marsac, N. and Houmard, J.: Complementary chromatic adaptation: Physiological conditions and action spectra, in: *Methods in Enzymology*, Academic Press, 318–328, 1988.
- Tarutani, K., Nagasaki, K., and Yamaguchi, M.: Viral impacts on total abundance and clonal composition of the harmful bloom-forming phytoplankton heterosigma akashiwo, *Appl. Environ. Microbiol.*, 66, 4916–4920, 2000.
- Thamatrakoln, K., Korenovska, O., Niheu, A. K., and Bidle, K. D.: Whole-genome expression analysis reveals a role for death-related genes in stress acclimation of the diatom *Thalassiosira pseudonana*, *Environ. Microbiol.*, 14, 67–81, 2012.
- Turk-Kubo, K., Frank, I., Hogan, M., Desnues, A., Bonnet, S., and Zehr, J.: Diazotroph community succession during the VAHINE mesocosms experiment (New Caledonia Lagoon), *Biogeosciences* 12, 7435–7452, doi:10.5194/bg-12-7435-2015, 2015.
- Van Mooy, B. A., Hmelo, L. R., Sofen, L. E., Campagna, S. R., May, A. L., Dyhrman, S. T., Heithoff, A., Webb, E. A., Mopper, L., and Mincer, T. J.: Quorum sensing control of phosphorus acquisition in *Trichodesmium* consortia, *The ISME Journal*, 6, 422–429, 2012.
- Van Wambeke, F., Pfreundt, U., Barani, A., Berthelot, H., Moutin, T., Rodier, M., Hess, W. R., and Bonnet, S.: Heterotrophic bacterial production and metabolic balance during the VAHINE mesocosm experiment in the New Caledonia lagoon, *Biogeosciences*, 13, 3187–3202, doi:10.5194/bg-13-3187-2016, 2016.
- Vardi, A., Berman-Frank, I., Rozenberg, T., Hadas, O., Kaplan, A., and Levine, A.: Programmed cell death of the dinoflagellate *Peridinium gatunense* is mediated by CO₂ limitation and oxidative stress, *Curr. Biol.*, 9, 1061–1064, 1999.
- Vardi, A., Haramaty, L., Van Mooy, B. A., Fredricks, H. F., Kimance, S. A., Larsen, A., and Bidle, K. D.: Host–virus dynamics and subcellular controls of cell fate in a natural coccolithophore population, *P. Natl. Acad. Sci.*, 109, 19327–19332, 2012.
- Walsby, A. F.: The properties and buoyancy providing role of gas vacuoles in *Trichodesmium*, *Brit. Phycol. J.*, 13, 103–116, 1978.
- Weitz, J. S. and Wilhelm, S. W.: Ocean viruses and their effects on microbial communities and biogeochemical cycles, *F1000 Biology Reports*, 4, 17, doi:10.3410/B4-17, 2012.
- Wu, Z., Jenkins, B. D., Rynearson, T. A., Dyhrman, S. T., Saito, M. A., Mercier, M., and Whitney, L. P.: Empirical bayes analysis of sequencing-based transcriptional profiling without replicates, *BMC Bioinformatics*, 11, 564, doi:10.1186/1471-2105-11-564, 2010.
- Zehr, J. P.: Nitrogen fixation in the Sea: Why Only *Trichodesmium*, in: *Molecular Ecology of Aquatic Microbes*, edited by: Joint, I., NATO ASI Series, Springer-Verlag, Heidelberg, 335–363, 1995.